

University of Alberta

Three-Dimensional Bookstein Shape Coordinates and Functional
Morphology of Passive Suspension Feeding in *Composita* (Brachiopoda,
Athyridida)

by

Benjamin Michael James Collins

A thesis submitted to the Faculty of Graduate Studies and Research
in partial fulfillment of the requirements for the degree of

Master of Science

Department of Earth and Atmospheric Sciences

©Benjamin Michael James Collins

Spring 2014

Permission is hereby granted to the University of Alberta Libraries to reproduce single copies of this thesis and to lend or sell such copies for private, scholarly or scientific research purposes only. Where the thesis is converted to, or otherwise made available in digital form, the University of Alberta will advise potential users of the thesis of these terms.

The author reserves all other publication and other rights in association with the copyright in the thesis and, except as herein before provided, neither the thesis nor any substantial portion thereof may be printed or otherwise reproduced in any material form whatsoever without the author's prior written permission.

ABSTRACT

The effects of shell morphology on passive fluid circulation are examined in Late Mississippian through Late Pennsylvanian *Composita* (Brachiopoda, Athyridida) from Texas, Kentucky, and Iowa. The first three-dimensional derivation of Bookstein shape coordinates is given in association with an in-depth discussion of the advantages and potential drawbacks of the technique for geometric shape analysis applications. Three-dimensional morphometric analysis of *Composita* shows a single shape distribution corresponding to progressive differentiation of the commissure into vertically displaced parasulcate, lateral, and sulcate gapes with increasing shell size, indicating an ontogenetic shape change trend. Gaping models of three specimens (including a simulated lophophore in the largest specimen) representative of different ontogenetic stages were used to observe the effects of morphology on passive flow circulation in a recirculating flume tank. All models showed medially-inhalant and laterally-exhalant passive circulation when oriented with the sulcus facing upstream, with more vigorous flow associated with increasing shell size.

ACKNOWLEDGEMENTS

First and foremost I would like to thank my advisor, Lindsey Leighton. His advice and encouragement were what made this project progress from an idea to a finished thesis. He has been a tremendous mentor and friend to me.

My committee members J.P. Zonneveld and Sally Leys provided invaluable suggestions and feedback that significantly improved this project. I thank them for opening my mind to new aspects of natural history.

Darrin Molinaro and Carrie Tyler collaborated with me on major parts of this research. Their involvement in this project was substantial, and helped me greatly exceed what I might have accomplished working on my own.

I thank my friends and colleagues who have helped create a fun and intellectual lab environment: Chris Schneider, Kristina Barclay, Emily Stafford, Frank Forcino, Amelinda Webb, and Cory Redman.

Funding for this research was provided by an NSERC Canada Graduate Scholarship, University of Alberta Walter H. Johns Graduate Fellowship, Geological Society of America Graduate Student Research Grant, Yale Peabody Museum of Natural History Charles Schuchert and Carl O. Dunbar Grant-in-Aid for Invertebrate Paleontological Research, Queen Elizabeth II Canada Graduate Scholarship, and a Paleontological Society Student Grant Award.

TABLE OF CONTENTS

Introduction	1
References	4
Chapter 1: Three-Dimensional Bookstein Shape Coordinates	6
Introduction	6
Theory and Application of Shape Coordinate Techniques	11
Bookstein Shape Coordinates	13
Three-Dimensional Landmark Coordinates	16
Three-Dimensional Bookstein Shape Coordinates	19
Discussion	20
Conclusions	23
References	30
Chapter 2: Functional Morphology of Passive Suspension Feeding in <i>Composita</i> (Brachiopoda, Athyridida)	33
Introduction	33
Background Theory	37
Specimen Selection and Morphometric Methods	41
Specimens	41
Morphometric Methods	41
Results (Morphometric Analysis)	44
Size and Shape Changes	44

Model Construction and Flume Testing Protocols	45
Model Construction	45
Flume Schematics and Testing Protocols	49
Results (Flume Tank Analysis)	52
Hollow Model Flow Patterns	52
Lophophore Model Flow Patterns	54
Discussion	55
Conclusion	62
References	84
Conclusions	91

LIST OF FIGURES

CHAPTER 1

Figure 1.1:

Examples of type one, two, and three landmarks.

24

Figure 1.2:

Hypothetical landmark-based morphometric analysis of a bivalve.

25

Figure 1.3:

Location of landmarks in Euclidean space.

26

Figure 1.4:

Rescaled landmark locations (Bookstein shape coordinates) in 1x1
shape coordinate space.

27

Figure 1.5:

Landmark data required for three-dimensional shape analysis.

28

Figure 1.6:

Components required to solve for the Cartesian coordinates of
landmark D, D_x , D_y , and D_z .

29

CHAPTER 2:

Figure 2.1:

The effect of viscous entrainment.

64

Figure 2.2:

Landmarks used for morphometric analysis of *Composita*.

65

Figure 2.3:

Z and X shape coordinates of landmark D.

66

Figure 2.4:

Z and Y shape coordinates of landmark D.

67

Figure 2.5:

Size and shape variation among samples of *Composita*.

68

Figure 2.6:

Allometric growth in *Composita*.

70

Figure 2.7:

Specimens of *Composita* used to construct models for use in flume tank experiments.

72

Figure 2.8:

Specimens, models, and model components used in flume experiments.

74

Figure 2.9:

Articulated specimen of *Composita* with external mold of spiralia preserved inside the shell; large model of *Composita* with simulated lophophore installed.

75

Figure 2.10:

Flume tank used for study of passive flow in *Composita*.

76

Figure 2.11:

Small hollow model of *Composita* showing medially-inhalant and laterally-exhalant passive flow (0.06 m/s unidirectional current).

77

Figure 2.12:

Intermediately-sized hollow models showing medially-inhalant and laterally-exhalant passive flow (0.06 m/s unidirectional current).

78

Figure 2.13:

Large hollow model showing medially-inhalant and laterally-exhalant passive flow, with vigorous outflow from both

parasulci (0.06 m/s unidirectional current).

79

Figure 2.14:

Large hollow model showing laterally-inhalant (upstream) and laterally-exhalant (downstream) passive flow (0.06 m/s unidirectional current).

80

Figure 2.15:

Large model with simulated lophophore installed. Note streamlined medially-inhalant and laterally-exhalant passive flow (0.06 m/s unidirectional current).

81

Figure 2.16:

Generalized ontogenetic pathways and brachial axis geometries of rhynchonelliform brachiopod lophophores.

82

ABBREVIATIONS

YPM: Yale Peabody Museum of Natural History.

INTRODUCTION

Marine animals from many phyla subsist by suspension feeding - the process of capturing and consuming food particles entrained in the water column (LaBarbera, 1984). Although many suspension feeding animals are capable of actively pumping water to generate feeding currents, actively induced fluid circulation is metabolically expensive (Leys *et al.*, 2011), and potentially inefficient in circumstances where animals cannot pump in a manner that augments ambient flow regimes. The general morphology of sessile suspension feeders such as brachiopods and sponges is known to significantly influence their feeding efficiency by enhancing induced (passive) fluid circulation (Vogel, 1974; LaBarbera, 1977), augmenting and potentially significantly reducing the need to actively pump water. The purpose of this study is to investigate the functional morphology of passive suspension feeding in the athyridide hbrachiopod genus *Composita*. In particular, the main underlying hypothesis of the study is that the shell morphology of *Composita* functioned as an effective passive suspension feeding body plan. Morphology and function are the two most important aspects of this work, and will effectively define the order in which it is presented.

Many species of *Composita* have been described from the Upper Devonian through Permian strata of the North American Mid-Continent, where the taxon occurs in great abundance (Grinnell and Andrews, 1964;

Lutz-Garihan, 1976). Although morphological variation is apparent in *Composita* throughout its stratigraphic range, general similarities among North American examples of the taxon have resulted in divergent classifications, with some workers grouping all forms within *Composita subtilita* (Sutherland and Harlow, 1967), or recognizing intergradational morphotypes of *Composita subtilita* (Burk, 1954; Lutz-Garihan, 1976). Regardless of classification, the hypothesis that the shell morphology of *Composita* functioned as an effective passive suspension feeding body plan depends on the nature of morphological variation in the taxon on both evolutionary and ontogenetic time scales. Chapter One ("Three-dimensional Bookstein Shape Coordinates") presents a three-dimensional extension of Bookstein shape coordinates (Bookstein, 1986, 1991), and includes a detailed discussion of the advantages and caveats of the method in geometric shape analysis applications.

Three-dimensional Bookstein shape coordinates are used for a morphometric analysis of *Composita* in the first half of Chapter Two ("Functional Morphology of Passive Suspension Feeding in *Composita* (Brachiopoda, Athyridida)"), which also forms the basis for a series of fluid dynamic experiments presented therein. The morphometric analysis of *Composita* addresses evolutionary and ontogenetic changes in shell morphology by incorporating samples inclusive of the majority of the size distribution and stratigraphic range of the taxon. Combined with

stratigraphic information, shape and size data from the morphometric analysis provide a quantitative depiction of morphological variation and changes in *Composita* throughout its ontogeny and evolutionary history.

The ultimate goal of this study is to test whether or not shells of *Composita* functioned to passively induce fluid circulation. The hypothesis of the study therefore not only depends on the nature of morphological variation in *Composita*, but also on the manner in which differences in shell shape relate to passively induced current circulation. The second half of Chapter Two presents a series of fluid dynamics experiments comparing passive circulation function among different morphotypes of *Composita* selected based on morphometric data, using 1:1 scale models of well-preserved representative specimens.

References:

Bookstein, F. L. 1986. Size and shape spaces for landmark data in two dimensions. *Statistical Science* 1:181-242.

Bookstein, F. L. 1991. *Morphometric tools for landmark data: geometry and biology*, Cambridge University Press, Cambridge.

Burk, C. A. 1954. Faunas and age of the Amsden Formation in Wyoming. *Journal of Paleontology* 28:1-16.

Grinnell, R. S., and G. W. Andrews. 1964. Morphologic studies of the brachiopod genus *Composita*. *Journal of Paleontology* 38:227-248.

LaBarbera, M. 1977. Brachiopod orientation to water movement 1. Theory, laboratory behavior, and field orientations. *Paleobiology* 3:270-287.

LaBarbera, M. 1984. Feeding currents and particle capture mechanisms in suspension-feeding animals. *American Zoologist* 24:71-84.

Leys, S. P., G. Yahel, M. A. Reidenbach, V. Tunnicliffe, U. Shavit, and H.

Reiswig. 2011. The sponge pump: the role of current induced flow in the design of the sponge body plan. PLoS ONE e27787

Lutz-Garihan, A. B. 1976. *Composita subtilita* (Brachiopoda) in the Wreford megacyclothem (Lower Permian) in Nebraska, Kansas, and Oklahoma. The University of Kansas Paleontological Contributions. Paper 81. 21 p.

Sutherland, P. K., and F. H. Harlow. 1967. Late Pennsylvanian brachiopods from north-central New Mexico. Journal of Paleontology 41:1065-1089.

Vogel, S. 1974. Current-induced flow through the sponge, *Halichondria*. The Biological Bulletin 147:443-456.

CHAPTER ONE: THREE-DIMENSIONAL BOOKSTEIN SHAPE COORDINATES

Introduction:

Morphometrics entails the quantitative analysis of form. All morphometric techniques attempt to provide statistically robust assessments of shape variation within and among different samples of organisms or objects. Capturing geometric information about shape variation has presented logistical and mathematical challenges to the field of morphometrics, resulting in the emergence of a variety of approaches to morphometric analysis (Rohlf and Marcus, 1993). Although sophisticated shape analysis techniques have been applied to diverse two-dimensional data (for example: Stone, 1998; Adams, 2004; Amaral et al., 2009), application of these methods to three-dimensional problems has been less widespread (for example: Monteiro-Filho et al., 2002; Loy et al., 2011), perhaps due to the mathematical obstacles associated with extending the thin-plate spline analogy for deformations into three dimensions (Bookstein, 1989). The purpose of this paper is to present a three-dimensional extension of Bookstein shape coordinates (Bookstein 1986, 1991), a geometric morphometric technique that has considerable utility for visualizing shape configurations and identifying shape changes between forms (Corti, 1993). Geometric morphometric methods differ from other morphometric approaches in that geometric shape analysis

techniques are based on comparisons of constellations of landmarks in which the relative spatial relationships among all of the landmarks are retained in their respective coordinate values.

The techniques presented here are logically advantageous, as primary data collection requires only linear caliper measurements: digitization of landmark coordinates from images is not required, nor is the use of expensive and platform-specific three-dimensional scanning equipment. This method is thus likely to be of particular benefit in field studies involving living specimens. Although the primary focus of the manuscript is the derivation of shape coordinates in three dimensions, for ease of use, a trigonometric solution for solving the x, y, and z coordinates of landmarks in Euclidean space is provided.

Two-dimensional morphometric techniques have a wide range of potential uses, and are tremendously valuable for examining features that appear in outline, or that are essentially constrained along a single plane. Two-dimensional techniques, however, may yield inaccurate results when applied to morphological problems that are inherently three-dimensional, as fundamentally different results and interpretations can be made when using data collection protocols more appropriate for three-dimensional features. For example, early morphometric investigations of the Cenozoic bivalves *Chione erosa* and *Chione cancellata* (a putative evolutionary lineage) using linear measurements digitized from two-dimensional

images portrayed a pattern of strong evolutionary stasis (Stanley and Yang, 1987). Later examination of the lineage, using caliper measurements of many of the same features in three dimensions, demonstrated significant morphological differences between the same two species (Roopnarine, 1995). The initial failure to identify these morphological differences may have resulted from the flattening of features, which when digitized in two-dimensional images, do not actually lie in the same plane in three dimensions, thereby introducing systematic error in size measurement data (Roopnarine, 1995). The potential for the introduction of similar systematic error is exacerbated in the case of objects that are more fundamentally three-dimensional. For instance, geometrically complex anatomical features, such as crania, are inherently three-dimensional in shape. Two-dimensional sections may not capture all of the significant components of shape variation in these features, and can therefore exclude important shape information from a morphometric analysis. Because studies explicitly examining morphological variance require information about the directionality as well as the magnitude of shape changes, three-dimensional morphometric techniques should be preferred for any analysis of forms and features that imply variance in three dimensions.

Contemporary morphometric methods, commonly referred to as geometric morphometric techniques, differ from traditional morphometric

approaches (Reymert et al., 1984) in that the former examine the relative positions of landmarks (two-dimensional or three-dimensional coordinates corresponding to specific, identifiable morphological points that coincide within or among specimens) in order to explicitly compare both local and uniform differences in form within and among samples. In the context of geometric morphometrics, shape refers to the spatial arrangement of a particular object, as represented by a series of landmarks, independent of information about its location, position in space, and size (Kendall, 1989). The goal of geometric shape analysis is to superimpose a set of objects within the same coordinate-space in order to depict how they differ in shape. For objects represented by a constellation of landmark coordinates, this procedure involves translating, scaling, and rotating their coordinate configurations according to some common metric. The class of shape analysis techniques commonly known as Procrustes methods includes a variety of approaches to superimposing constellations of landmark coordinates (Rohlf and Slice, 1990). Procrustes methods differ most in terms of the mathematical techniques employed to rotate and scale sets of coordinates, with translation typically performed by relocating the centroid, or geometric mean, of each coordinate constellation to a common location in space. The technique of Bookstein shape coordinates approaches superimposition of coordinate configurations in a manner fundamentally different from the various Procrustes methods. Bookstein

shape coordinates are calculated based on interlandmark measurements for triangular (in the case of two-dimensional coordinates) or tetrahedral (in the case of three-dimensional coordinates) configurations of landmarks. In both two and three dimensions, the technique eliminates size variation between specimens by uniformly scaling coordinate configurations according to a common baseline measure, demarcated by two landmarks common to all of the forms being studied. For two dimensional shape coordinates, assigning the common baseline to a fixed position (typically along the x-axis in Euclidean space) translates and rotates the coordinate configuration of every specimen to a common location and position in space. Three-dimensional shape coordinate configurations are translated and scaled in the same manner as two-dimensional shape coordinates, but are rotated to a common position by assigning a base plane shared among all specimens to a single specific Euclidean plane. Although previously only derived for landmarks with coordinates in two-dimensional space, three-dimensional Bookstein shape coordinates were used by Tyler and Leighton (2011) for analyses of morphological variation associated with character displacement in Ordovician brachiopods. Because meaningful landmark selection constitutes a fundamental aspect of any geometric morphometric study, a review of landmark types will precede our derivation of three-dimensional Bookstein shape coordinates.

Theory and Application of Shape Coordinate Techniques:

Geometric morphometric techniques use landmarks in order to provide a more informative depiction of organism form than can be achieved using non-spatially referenced data. Landmarks, in a purely biological sense, represent identifiable morphological points that coincide within, or between, forms. Assigning landmarks discrete coordinates in space provides a mathematical formalization of morphological distance, therefore allowing depictions of the relative spatial positions of specific features (Bookstein, 1991). The most obvious advantage of this formalization is the ease with which it becomes possible to directly observe changes in the positions of various landmarks with respect to one another. Because the relative positions of landmarks correspond to real spatial configurations, landmark data express actual variation in form rather than more abstract quantities such as ratios of lengths. Therefore, statistical differences in landmark configuration are directly representative of statistical differences in morphology.

Meaningful depictions of morphological variation depend on the selection and use of informative landmarks. Bookstein (1991) described three categories of landmarks, which can be practically thought of as reflecting different levels of morphological resolution:

(1) Type one landmarks: defined by distinct intersections at which

three morphological features coincide (Figure 1.1, landmark 1). Common examples include points demarcating junctions of maximum curvature with planes of symmetry, and triple junctions of elongate features, such as cranial sutures. Type one landmarks may represent biologically homologous features, and therefore have substantial utility for phylogenetic studies.

(2) Type two landmarks: defined by inflections of curves, that is, points of local maxima or minima (Figure 1.1, landmarks 2 and 3). Type two landmarks are often associated with functionally significant features such as points of articulation or dental cusps.

(3) Type three landmarks: defined by points delineating maximum dimensions of organisms or anatomical features (Figure 1.1, landmarks 4 and 5). In the strict sense, type three landmarks do not express information about shape in more than one dimension.

Type one landmarks can be thought of as having the greatest morphological resolution in the sense that their relative configurations capture the most information about local features of shape. In contrast, type three landmarks provide only very general information about shape, and only in a single dimension.

Although landmark selection is obviously dictated to some degree by the particular taxa being studied, landmarks should be chosen in order to best suit the hypothesis being tested. For instance, in functional studies,

landmarks are chosen to reflect a hypothesized relationship between specific morphological features (often representable by type two landmarks) and some functional variable(s). Within a single species, morphological change during ontogeny might be correlated with ecological phenomena on different spatial and temporal time scales, and probably has substantial functional significance. In these cases, type two landmarks are likely appropriate. Identifying differences between species is of fundamental importance in evolutionary studies, where patterns of morphological variation are often the most readily observable features defining common ancestry. Type one landmarks, often indicative of homologous features, are particularly well suited to such cases.

Bookstein Shape Coordinates:

Shape coordinate techniques treat landmarks as locations in Euclidean space (Rohlf and Marcus, 1993). A significant portion of this treatment involves defining a set of measurements common to all of the forms being studied that allows calculation of the landmark coordinates. The method of Bookstein shape coordinates accomplishes this task by defining a standardized baseline measurement (assigned to the x-axis in Euclidean space) relative to which the position of other landmarks can be calculated (Bookstein, 1986). Following the calculation of Cartesian coordinates in Euclidean space, landmarks are scaled to a common shape

coordinate space, defined according to the baseline measurement, eliminating size variation between samples.

Consider a situation, as shown in Figure 1.2, where changes in the general body form of an organism are of interest. Points A, B, and C are landmarks chosen to approximate the triangular shape of the bivalve. If, for example, it is hypothesized that the position of landmark C changes on an evolutionary time scale, it is necessary to compare the mean position of the landmark between samples of stratigraphically older and stratigraphically younger specimens in order to assess the degree of change. To compare the position of landmark C between specimens and samples in Euclidean space, a common baseline measure spanning a distance between two landmarks (in this case, the line **AB**) is defined. This distance becomes the x-axis common to all specimens in Euclidean space (Figure 1.3). After measuring the distance between each of the three defined landmarks, a series of calculations are required in order to determine the Cartesian coordinates of landmark C in Euclidean space: Beginning with the measurements **AB**, **AC**, and **BC**, which correspond to the distances between each of the three defined landmarks, the baseline measure (**AB**) is assigned to the x-axis. The angle subtended by line **AC** and the x-axis shall be defined as the variable θ_A (Figure 1.2). θ_A is related to the three defined measurements by the law of cosines, as follows:

$$\mathbf{BC}^2 = \mathbf{AC}^2 + \mathbf{AB}^2 - 2(\mathbf{AC})(\mathbf{AB})\cos(\theta_A)$$

Therefore:

$$\theta_A = \arccos[(AC^2 + AB^2 - BC^2) / 2(AC)(AB)]$$

Knowing \mathbf{AC} and θ_A , the polar coordinates of landmark C in Euclidean space, the equivalent Cartesian coordinates can be determined by the following transformations:

$$C_x = (AC)\cos(\theta_A)$$

$$C_y = (AC)\sin(\theta_A)$$

Given the Cartesian coordinates of landmarks A, B, and C, it is possible to observe an approximation of the size and shape of an individual specimen in Euclidean space. In order to make comparisons between groups of specimens that naturally vary in size, however, it is necessary to scale all of the specimens in our samples equally according to the common baseline measure, creating a shared shape coordinate space. Bookstein shape coordinates are calculated by dividing the Cartesian coordinates of each landmark by the length of the baseline measure along the x-axis. This procedure scales the baseline common to every specimen to unity, permitting direct graphical and statistical comparisons of specimens and samples (Figure 1.4). The resulting Bookstein shape coordinates, C_x' and C_y' , eliminate any variation in size between specimens, and therefore depict true differences in shape:

$$C_x' = (AC)\cos(\theta_A) / (AB)$$

$$C_y' = (\mathbf{AC})\sin(\theta_A) / (\mathbf{AB})$$

The power of this technique comes from the fact that it permits direct applications of multivariate tests of difference, such as Hotelling's T-squared test, to morphological data. In the life sciences, this allows comparison of shape variation amongst samples that might be organized so as to be temporally, spatially, and/or taxonomically independent. Therefore, if shape variation can be correlated with the performance of some functional variable, it is possible to test functional hypotheses on evolutionary and developmental time scales. In addition, as shown in Figures 2-4, the method allows for an intuitive visualization of organisms in shape coordinate space.

Three-Dimensional Landmark Coordinates:

In order to extend Bookstein shape coordinates into three-dimensional space, a base plane (analogous to the baseline in two-dimensional space) common to all of the forms being examined is selected (Figure 1.5). This plane (occupying part of the x-y Cartesian plane) is defined by three landmarks, the distance between two of which forms a scaling baseline along the x-axis (line **ab** in Figure 1.5). Recall that in two-dimensional space, the location of a given landmark is determined based on its position relative to the two landmarks that define the baseline measurement (Figures 1.3 and 1.4). In three-dimensional

space, the location of a given landmark is determined based on its position relative to the three landmarks that define the base plane.

Measurement of the distances between each of the landmarks defined for a collection of study specimens provides a basic set of data used to assign landmarks positions in Euclidean space (Figure 1.6). Three landmarks define the base plane, two of which are assigned positions on the x-axis (landmarks A and B, and the line **ab** in Figure 1.5). The Cartesian coordinates of the remaining landmarks (C and D in Figure 1.6) can then be determined as follows:

The Cartesian coordinates defining landmark C, C_x and C_y , are determined using the two-dimensional form of Pythagoras' theorem:

$$C_x^2 + C_y^2 = (ac)^2 \dots (1)$$

$$((ab) - C_x)^2 + C_y^2 = (bc)^2 \dots (2)$$

Rearranging, and expanding the left hand side of equation (2):

$$(ab)^2 - 2(ab)C_x + C_x^2 + C_y^2 - (bc)^2 = C_x^2 + C_y^2 - (ac)^2$$

which simplifies to:

$$2(ab)C_x = (ab)^2 + (ac)^2 - (bc)^2$$

therefore:

$$C_x = [(ab)^2 + (ac)^2 - (bc)^2] / 2(ab)$$

Knowing the value of C_x , equation (1) can be rearranged to give:

$$C_y = \sqrt{(ac)^2 - C_x^2}$$

Because landmark C lies within the x-y plane, $C_z = 0$.

The Cartesian coordinates defining landmark D, D_x , D_y , and D_z , are determined using the three-dimensional form of Pythagoras' theorem (Figure 1.6):

$$D_x^2 + D_y^2 + D_z^2 = (\mathbf{ad})^2 \dots (3)$$

$$((\mathbf{ab}) - D_x)^2 + D_y^2 + D_z^2 = (\mathbf{bd})^2 \dots (4)$$

$$(C_x - D_x)^2 + (D_y - C_y)^2 + D_z^2 = (\mathbf{cd})^2 \dots (5)$$

First, D_x is determined by rearranging equations (3) and (4):

$$((\mathbf{ab}) - D_x)^2 + D_y^2 + D_z^2 - (\mathbf{bd})^2 = D_x^2 + D_y^2 + D_z^2 - (\mathbf{ad})^2$$

simplifying, and expanding the left hand side:

$$(\mathbf{ab})^2 - 2(\mathbf{ab})D_x + D_x^2 - (\mathbf{bd})^2 = D_x^2 - (\mathbf{ad})^2$$

therefore:

$$D_x = [(\mathbf{ab})^2 + (\mathbf{ad})^2 - (\mathbf{bd})^2] / 2(\mathbf{ab})$$

Knowing D_x , equations (4) and (5) can simply be rearranged to solve for

D_y :

$$(C_x - D_x)^2 + (D_y - C_y)^2 + D_z^2 - (\mathbf{cd})^2 = (\mathbf{ab})^2 - 2(\mathbf{ab})D_x + D_x^2 + D_y^2 + D_z^2 - (\mathbf{bd})^2$$

simplifying, and expanding the left hand side:

$$C_x^2 - 2C_xD_x + D_x^2 + D_y^2 - 2D_yC_y + C_y^2 - (\mathbf{cd})^2 = (\mathbf{ab})^2 - 2(\mathbf{ab})D_x + D_x^2 + D_y^2 - (\mathbf{bd})^2 + (\mathbf{cd})^2$$

simplifying and rearranging:

$$2D_yC_y = C_x^2 - 2C_xD_x + C_y^2 - (ab)^2 + 2(ab)D_x + (bd)^2 + (cd)^2$$

therefore:

$$D_y = [C_x^2 - 2C_xD_x + C_y^2 - (ab)^2 + 2(ab)D_x + (bd)^2 + (cd)^2] / 2C_y$$

Knowing the values of D_x and D_y , equation (3) can be rearranged to solve

for D_z :

$$D_z = \sqrt{(ad)^2 - D_x^2 - D_y^2}$$

Three-Dimensional Bookstein Shape Coordinates:

Three-dimensional shape coordinate spaces are defined by scaling the x-axis dimension of the base plane (line **ab** in Figures 1.5 and 1.6) to unity, and equally scaling the Cartesian coordinates of the other landmarks according to this dimension. The resulting Bookstein shape coordinates of landmarks C and D are therefore determined as follows:

$$C_x' = [(ab)^2 + (ac)^2 - (bc)^2] / 3(ab)$$

$$C_y' = \sqrt{(ac)^2 - C_x'^2} / (ab)$$

$$D_x' = [(ab)^2 + (ad)^2 - (bd)^2] / 3(ab)$$

$$D_y' = \{[C_x^2 - 2C_xD_x + C_y^2 - (ab)^2 + 2(ab)D_x + (bd)^2 + (cd)^2] / 2C_y\} / (ab)$$

$$D_z' = \{\sqrt{(ad)^2 - D_x'^2 - D_y'^2}\} / (ab)$$

As a result, one of the landmarks comprising the base plane (landmark C in Figures 1.5 and 1.6), although lying on the x-y plane, may be compared

between specimens and samples in a meaningful way. Landmarks A and B, which lie along the x-axis, by definition have Bookstein shape coordinates of (0, 0, 0) and (1, 0, 0), respectively.

Although shape coordinate spaces are defined by scaling a baseline measure to unity, and therefore do not allow for biologically or statistically meaningful comparisons of those landmarks that define the baseline, all of the spatial information related to the relative positions of each of the landmarks being observed is contained in the standardized (shape coordinate space) positions of the non-baseline Bookstein shape coordinates. As shown above, the position of a given landmark in shape coordinate space is determined simply by dividing all of its coordinates by the original dimension of the scaling baseline (line **ab** in Figure 1.5). This operation is equivalent to multiplying a series of vectors (that is, the Cartesian coordinates of each landmark) by a uniform scaling matrix, which thereby preserves all of the spatial relationships that define the landmark configuration of the original specimen.

Discussion:

Bookstein shape coordinates have the advantage of providing a direct visualization of landmark configurations for large samples of specimens, which can be easily used to map changes in mean configurations between different samples (Corti, 1993). Extending this

methodology into three dimensions greatly expands the variety of morphological features that can be examined, and enables more detailed depictions of shape change. The main drawback of this technique is the fact that differences or changes in the configuration of the baseline shape coordinates are not visually or statistically detectable. Although spatial information about the *relative* position of these coordinates is preserved in the locations of the non-baseline landmarks, distinguishing differences in the configuration of the baseline coordinates is not possible using the Bookstein shape coordinates method alone. However, many potential applications exist in which changes in the configuration of baseline landmarks do not have significant bearing on the features being examined. Shape changes for features demarcated by type two landmarks, which are often functionally significant, are good examples of such cases. Choosing baselines defined by type one landmarks that can be reasonably expected to show minimal shape change between samples (such as the junction of a plane of symmetry with normal bone sutures) can also avoid this problem to some extent.

An important consequence of the mathematical methodology used to calculate three-dimensional Bookstein shape coordinates is the fact that the three landmarks used to define a base plane are forced to lie within a horizontal plane in Euclidean space. The result of this convention is that graphs of shape coordinates imply a horizontal base plane, which may not

represent its real orientation with respect to the organisms or objects being studied. As with choosing an adequate baseline, base plane landmark selection is non-trivial, and should ideally involve features that can be expected to show negligible variation between samples. Additionally, choosing base plane landmarks that actually approximate a real horizontal plane on the object can make graphical depictions of shape variation in the landmarks that do not define the base plane less abstract.

Corti (1993) argued that Bookstein shape coordinates should be considered as a basic, or first-order technique for studying patterns of shape change. In this sense, the technique provides a useful exploratory tool for problems that might later benefit from treatment using more conceptually complex methods such as those from warp analysis (e.g., Slice, 2007). However, in many cases, Bookstein shape coordinates allow direct testing of hypotheses involving shape variation. Multivariate tests of difference, such as Hotelling's T-squared test, can be applied directly to shape coordinate data to determine if independent samples differ significantly under various conditions or treatments. If significant differences in shape exist, principal component analysis can be used to detect what landmarks have the most important effect on shape variation between samples. Discriminant analysis can be used in conjunction with these techniques to assess the directionality of morphological changes, which is essential for making unambiguous interpretations about the

external factors driving shape variation (Tyler and Leighton, 2011).

Conclusions:

Three-dimensional morphometric techniques are preferable for studies of geometrically complex morphological features that show shape variation in three dimensions. Bookstein shape coordinates provide an effective and logically convenient approach to three-dimensional morphometric analysis. The ease with which preliminary data can be collected makes the method a practical choice for field studies, and particularly for research involving living specimens, as no specialized imaging or digitization equipment is required to calculate landmark coordinates. Differences among complex forms are easily recognizable in three-dimensional shape coordinate space, and a variety of statistical techniques can be directly applied to shape coordinate data, providing a robust depiction of shape variation between samples, and enabling numerous hypothesis testing applications.

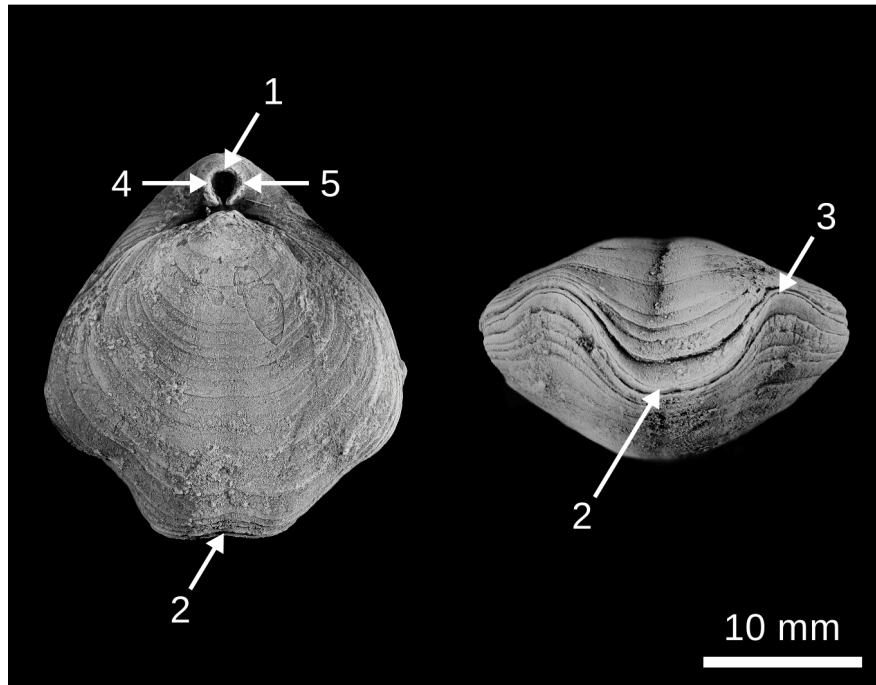


Figure 1.1:

Examples of type one (arrow 1), two (arrows 2 and 3), and three (arrows 4 and 5) landmarks in the Paleozoic brachiopod *Composita* (YPM 147214). Arrow 1 demarcates the intersection of the plane of bilateral symmetry with the posterior-most point of the pedicle foramen. Arrows two and three demarcate the dorsal-most point of the anterior medial sulcus and the ventral-most point of the parasulcus along the shell commissure, respectively; both landmarks are local maxima of curvature associated with accretionary growth of the shell. Arrows 4 and 5 demarcate the largest dimension of the pedicle foramen perpendicular to the plane of bilateral symmetry (because the pedicle foramen is circular, it does not have local maxima or minima of curvature).

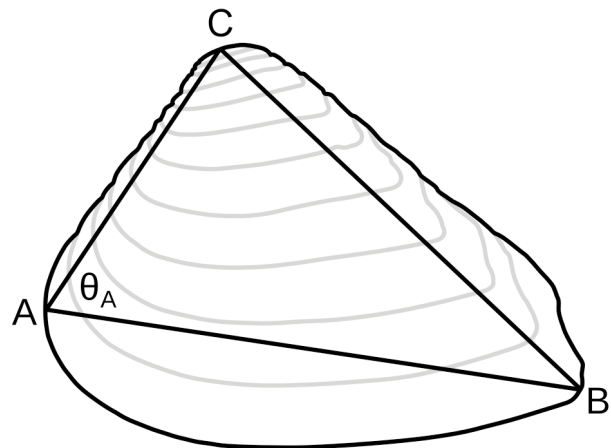


Figure 1.2:

Hypothetical landmark-based morphometric analysis of a bivalve.

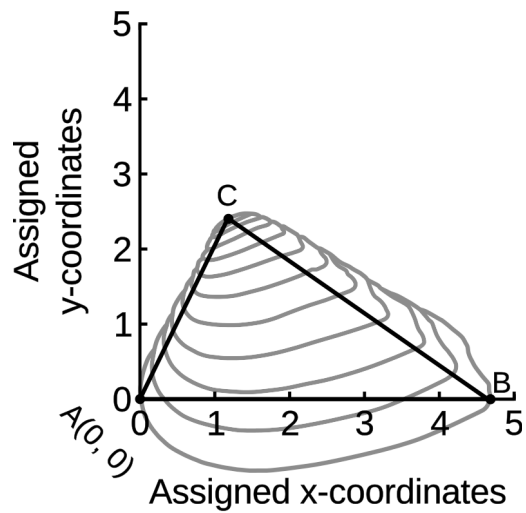


Figure 1.3:

Location of landmarks in Euclidean space. The line segment spanning the distance between landmarks A and B is assigned to the x-axis. The Cartesian coordinates of landmark C are determined by a series of calculations shown in the text.

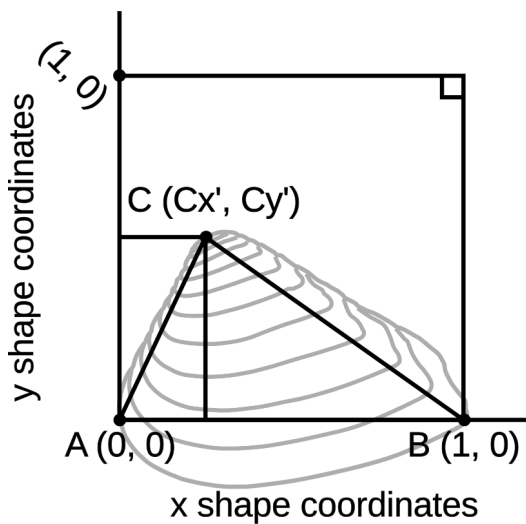


Figure 1.4:

Rescaled landmark locations (Bookstein shape coordinates) in 1×1 shape coordinate space.

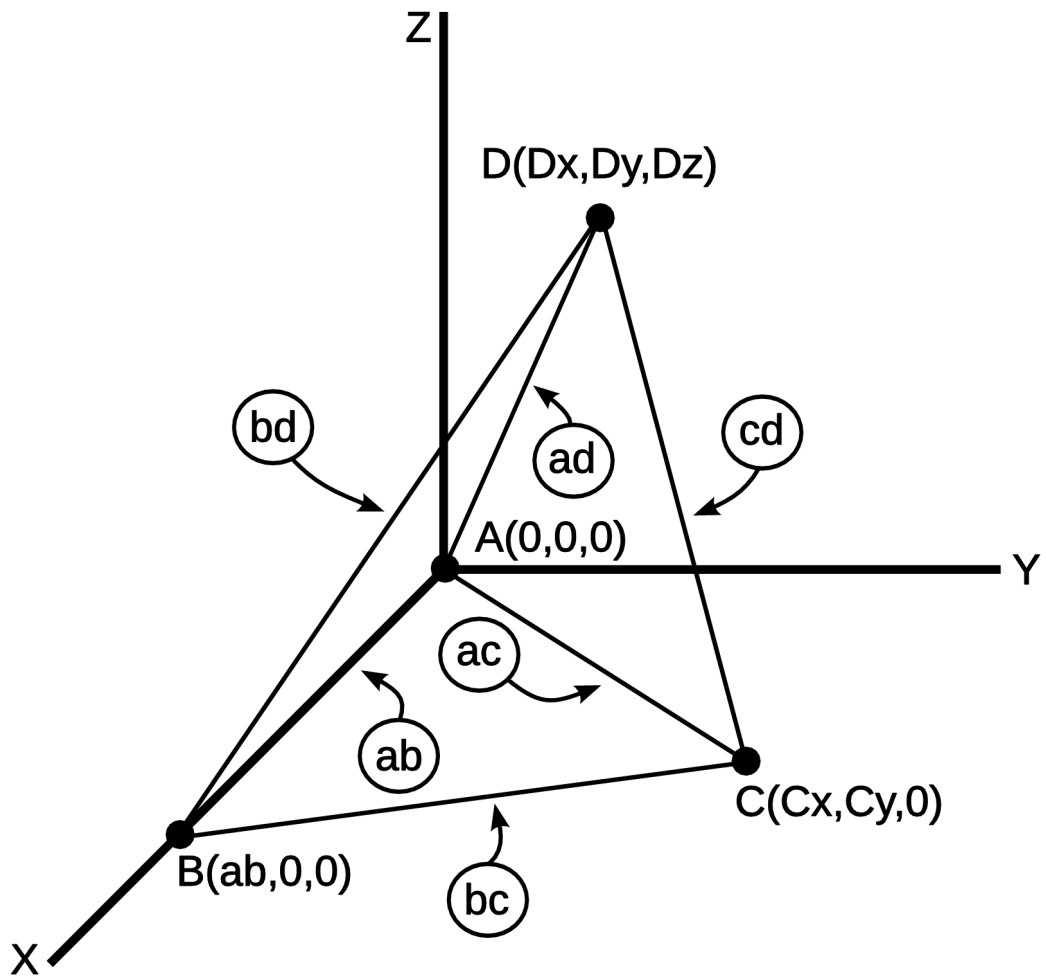


Figure 1.5:

Landmark data required for three-dimensional shape analysis. The dimensions of lines ab, ac, ad, bc, bd, and cd are determined by measurement of the distances between each pair of landmarks. Landmarks A and B, and therefore the line ab, are assigned to the x-axis in Euclidean space.

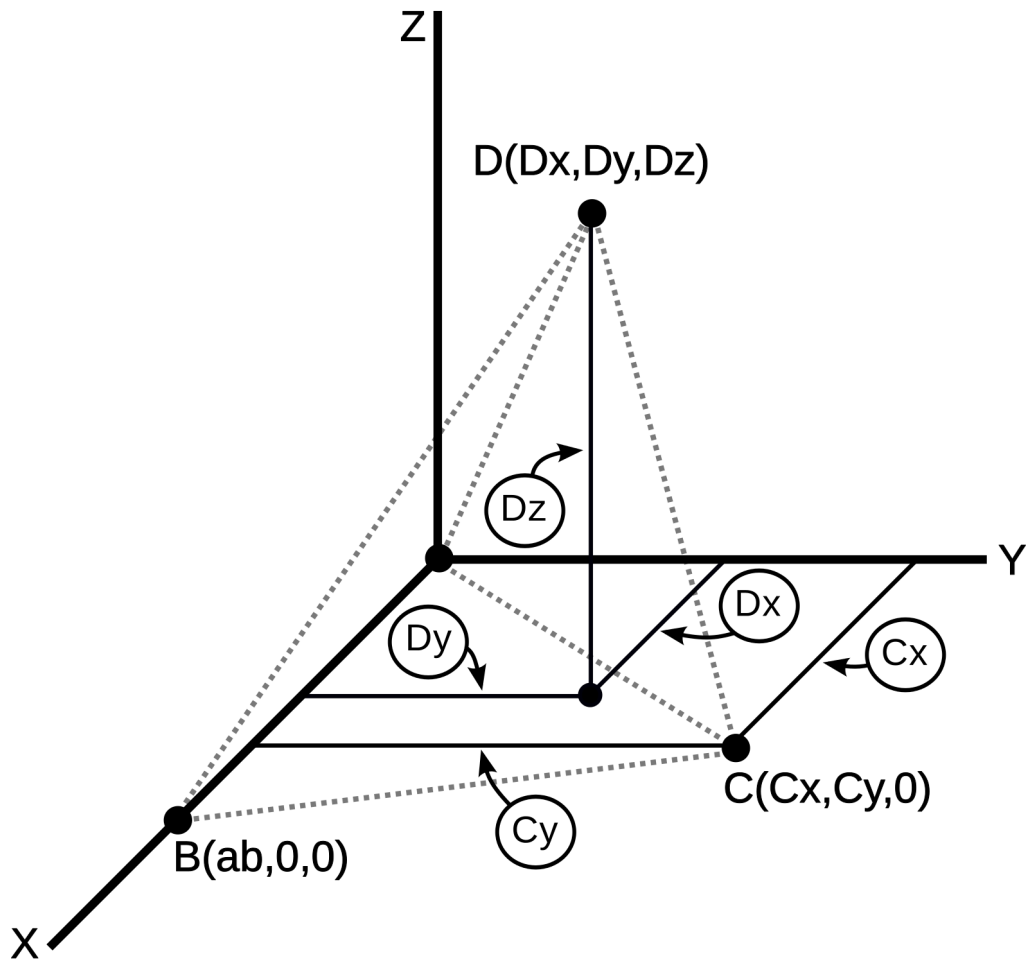


Figure 1.6:

Components required to solve for the Cartesian coordinates of landmark D, D_x , D_y , and D_z .

References:

Adams, D. C. 2004. Character displacement via aggressive interference in Appalachian salamanders. *Ecology* 85:2664-2670.

Amaral, A. R., M. M. Coelho, J. Marugan-Lobon, and F. J. Rohlf. 2009. Cranial shape differentiation in three closely related delphinid cetacean species: insights into evolutionary history. *Zoology* 112:38-47.

Bookstein, F. L. 1986. Size and shape spaces for landmark data in two dimensions. *Statistical Science* 1:181-242.

Bookstein, F. L. 1989. Principal warps: thin-plate splines and the decomposition of deformations. *IEEE Transactions on Pattern Analysis and Machine Intelligence* 11:567-585.

Bookstein, F. L. 1991. *Morphometric tools for landmark data: geometry and biology*, Cambridge University Press, Cambridge.

Corti, M. 1993. Geometric morphometrics: an extension of the revolution. *Trends in Ecology and Evolution* 8:302-303.

Kendall, D. G. 1989. A survey of the statistical theory of shape. *Statistical Science* 4:87-120.

Loy, A., A. Tamburelli, R. Carlini, and D. E. Slice. 2011. Craniometric variation of some Mediterranean and Atlantic populations of *Stenella coeruleoalba* (Mammalia, Delphinidae); a three-dimensional geometric morphometric analysis. *Marine Mammal Science* 27:E65-E78.

Monteiro-Filho, E. L. A., L. R. Monteiro, and S. F. Reis. 2002. Skull shape and size divergence in dolphins of the genus *Sotalia*: a tridimensional morphometric analysis. *Journal of Mammalogy*. 83:125-134.

Reyment, R. A., R. E. Blackith, and N. A. Campbell. 1984. *Multivariate Morphometrics*, Academic Press, New York.

Rohlf, F. J. and L. F. Marcus. 1993. A revolution in morphometrics. *Trends in Ecology and Evolution* 8:129-132.

Rohlf, F. J. and D. Slice. 1990. Extensions of the Procrustes method for the optimal superposition of landmarks. *Systematic Zoology*

39:40-59.

Roopnarine, P. D. 1995. A re-evaluation of evolutionary stasis between the bivalve species *Chione erosa* and *Chione cancellata* (Bivalvia: Veneridae). *Journal of Paleontology* 69:280-287.

Slice, D. E. 2007. Geometric morphometrics. *Annual Review of Anthropology* 36:261-281.

Stanley, S. M. and X. Yang. 1987. Approximate evolutionary stasis for bivalve morphology over millions of years: a multivariate multilineage study. *Paleobiology* 13:113-139.

Stone, J. R. 1998. Landmark-based thin-plate spline relative warp analysis of gastropod shells. *Systematic Biology* 47:254-263.

Tyler, C. L. and L. R. Leighton. 2011. Detecting competition in the fossil record: support for character displacement among Ordovician brachiopods. *Palaeogeography, Palaeoclimatology, Palaeoecology* 307:205-217.

CHAPTER TWO: FUNCTIONAL MORPHOLOGY OF PASSIVE
SUSPENSION FEEDING IN COMPOSITA (BRACHTIOPIODA,
ATHYRIDIDA)

Introduction:

The ecology and evolution of all organisms is strongly associated with the morphological and physiological limitations that influence their distribution and function. Therefore, understanding how different life modes and subsistence strategies influence the evolution of novel body plans and morphological features is fundamentally important for identifying the biotic and abiotic factors that govern the long term structure and diversity of ecosystems. Throughout the Phanerozoic Eon, suspension feeding has been a common subsistence strategy for marine organisms, especially benthic invertebrates. Although some suspension feeding animals have evolved biological pumping systems that allow them to actively circulate fluid, continuous active circulation (generally known as active suspension feeding) requires a large expenditure of metabolic energy (Leys *et al.*, 2011). However, many animals capable of active suspension feeding are also able to passively induce fluid circulation by orienting themselves in a particular manner with respect to ambient flow, consequently increasing pumping efficiency and reducing metabolic expenses (Vogel and Bretz, 1972). Passive suspension feeding requires that an animal possess a streamlined body plan that can effectively

function to induce and redirect flow. Modern brachiopods have been observed to reorient their shells while feeding in response to changes in the direction of ambient flow (LaBarbera, 1977). These observations suggest that the shells of brachiopods have an important functional relationship with suspension feeding, and potentially allow these animals to passively suspension feed. The purpose of this paper is to test the hypothesis that the shell morphology of the athyridide brachiopod *Composita* functioned as an effective passive suspension feeding body plan.

Composita is a ubiquitous fossil in the Upper Devonian (Famennian) through Permian (latest Guadalupian) strata of the North American Mid-Continent (Lutz-Garihan, 1976), is found in strata representative of a broad range of paleoenvironmental conditions (Leighton and Schneider, 2008), and is a member of the long-ranging (Famennian - Changhsingian), cosmopolitan athyridide subfamily Spirigerellinae (Alvarez *et al.*, 1998). Numerous species of *Composita* have been described from North America (for a detailed review see Grinnell and Andrews, 1964), however, strong morphological similarities among these supposed species have led some workers to group all forms of the genus within the species *Composita subtilita* (Sutherland and Harlow, 1967), or define a series of intergrading varieties or morphotypes of *Composita subtilita* (Burk, 1954; Lutz-Garihan, 1976). Due to the fact

that North American examples of *Composita* have typically been described on the basis of ambiguous qualitative characters, and appear difficult to separate even on the basis of typical dimensional measurements (Grinnell and Andrews, 1964; Sutherland and Harlow, 1967), this study did not attempt to identify any samples of the taxon to the species level prior to morphometric analysis.

The hypothesis that the shell morphology of *Composita* functioned as an effective passive suspension feeding body plan has an important underlying caveat. Qualitative morphological variation is apparent in *Composita* throughout its entire stratigraphic range (Grinnell and Andrews, 1964; Lutz-Garihan, 1976), however, due to the different approaches to classification that have been applied in describing and identifying forms of the genus, it is unclear how these differences relate to the evolutionary and ontogenetic history of the taxon. As the ability of an organism to passively circulate fluid relies strongly on its shape, evolutionary and/or ontogenetic changes in the shell morphology of *Composita* have significant bearing on the hypothesis of this study. Both of these aspects were controlled for by using a three-dimensional geometric morphometric analysis to test for shape and size differences among samples of *Composita* representative of the majority of its size distribution (to control for possible ontogenetic changes) and stratigraphic range (to control for possible evolutionary changes). The purpose of this analysis was to

determine: (1) If differences in external shape were apparent in *Composita* using unambiguous quantitative measures; (2) If differences in shape did exist, whether they were more strongly associated with relative shell size (implying possible ontogenetic change) or stratigraphic position (implying possible evolutionary change); and (3) How differences in shell morphology might relate to passive suspension feeding function.

From both an evolutionary and developmental perspective, tests of function serve to establish the degree to which morphological variation is related to specific functional properties of organisms (Alexander, 2001). Therefore, the validity of the hypothesis that the shell morphology of *Composita* functioned as an effective passive suspension feeding body plan is contingent upon both the nature of variation in its shell shape (the direction and magnitude of shape change, as well as its relationship with the evolutionary and ontogenetic history of the taxon), and the relationship between this variation and relative passive feeding performance. One of the main applications of morphometric data is in identifying the range of morphological variation shown by a taxon. For this study, shape and size distributions resulting from the morphometric analysis were used to select a series of specimens found to reflect the range of variation in shell morphology shown by *Composita*. The selected specimens were used to build 1:1 scale articulated models suitable for comparing the relative fluid circulation performance of the different shell morphologies in a flume tank.

The purpose of these tests was to determine: (1) how variation in shell shape affected passive flow circulation; (2) how shell orientation with respect to the direction of ambient current affected passive flow circulation; and (3) how differences in relative fluid circulation performance relate to the evolutionary and ontogenetic history of *Composita*.

Although previous investigations of flow patterns around model brachiopod shells (Wallace and Ager, 1966; Alexander, 1999; Shiino *et al.*, 2009; Shiino, 2010) have used similar protocols to demonstrate the effects of shell morphology and orientation on passive flow circulation, no prior studies have examined the relative performance of forms representative of different stages in the evolutionary or ontogenetic history of a taxon. Additionally, no previous studies of passive feeding in extinct brachiopods have attempted to account for the resistance to ambient flow that would have been caused by the feeding organs of the living organisms. To replicate some degree of this resistance, a simulated lophophore was constructed for testing with the largest brachiopod model used in this study (see Model Construction and Flume Testing Protocols).

Background Theory:

The main physical process thought to be responsible for inducing passive flow in benthic suspension feeding animals is the phenomenon of viscous entrainment (Vogel and Bretz, 1972; Vogel, 1974, 1994). Viscosity,

or the tendency of fluids to resist deformation due to shear stress, produces velocity gradients in flows where they encounter boundaries with solid surfaces, such as at interfaces with channel walls or substrates (Figure 2.1). These velocity gradients form as a result of a property of viscous fluids known as the no-slip condition (Prandtl and Tietjens, 1934). The no-slip condition states that the velocity of a moving fluid at its interface with a solid is equal to the velocity of the solid. This property is responsible for the effects of drag. Simply put, the same internal friction that causes viscous fluids to resist deformation due to shear stress also causes them to adhere to solid surfaces. Within a moving fluid, the area in the vicinity of a solid surface in which viscosity has an effect on flow, and where a vertical velocity gradient is present (Figure 2.1), is called the boundary layer. Moving away from the fluid-solid interface, velocity increases asymptotically due to decreasing friction (Vogel, 1994). The zone of greatest flow velocity, in which the presence of the solid body has no discernible effect on flow, is referred to as the free stream. Living in the boundary layer, within or attached to the substrate, is of considerable advantage to suspension feeding organisms. As per the no-slip condition, flow velocity at the substrate is zero. Therefore, any organism with a body plan approximating a simple vertically-oriented conduit system can exploit the energy potential that exists due to the higher flow velocities occurring further away from the substrate (Vogel, 1974). As shown in Figure 2.1,

fluid inside of a pipe with one opening positioned near the substrate and another opening located further up in the boundary layer will tend to be sucked out through the higher end of the pipe due to the greater flow velocity in its vicinity. This is the effect of viscous entrainment.

While alive, a pedunculate, biconvex brachiopod such as *Composita* would likely have positioned itself with its pedicle foramen (Figure 2.2) resting flush against the substrate, or close to it. As a result, the convexity of the dorsal valve (the underside of typical biconvex brachiopods in life position) would tend to incline the shell such that its anterior end would generally be positioned higher above the substrate than each lateral side. However, *Composita* has a geometrically complex commissure, with a deep dorsally-oriented fold and sulcus (landmark B in Figure 2.2) flanked on each side by a less pronounced, ventrally-oriented parasulcus (landmark D in Figure 2.2). Therefore, with the shell gaping in life position, the deep medial sulcus gape would be located closer to the substrate than each lateral gape and parasulcus gape unless the animal was attached at an angle closely approaching 90 degrees (unlikely due to the posterior convexity of the ventral valve). Due to viscous entrainment, any suspension feeding organism with well defined, vertically displaced inhalant and exhalant openings should be predisposed to passive exploitation of ambient flow. As shown in Figure 2.2, *Composita* was able to produce medial and lateral openings that were vertically displaced from

one another while gaping. Therefore, viscous entrainment should tend to cause ambient flow to circulate through the brachiopod by entering the shell via the medial sulcus (presumably located closer to the substrate), and exiting through each lateral gape and parasulcus (located higher above the substrate). The opposite pattern would be expected in the case of biconvex brachiopods with flatter commissures and/or shallower sulci. Indeed, living *Laqueus californianus*, *Terebratulina unguicula*, *Terebratalia transversa*, and *Hemithyris psittacea* all show laterally inhalant and medially exhalant feeding current patterns (LaBarbera, 1977).

Medially inhalant and laterally exhalant passive flow patterns have been experimentally demonstrated in hollow models of the spiriferide brachiopods *Paraspirifer bownockeri* and *Cyrtospirifer* (Wallace and Ager, 1966; Alexander, 1999; Shiino *et al.*, 2009; Shiino, 2010). Although neither of these taxa are parasulcate, both possess deep medial sulci and convex dorsal valves (in both *Paraspirifer* and *Cyrtospirifer*, much of this convexity is due to the strong expression of the sulcus along the midline of the dorsal valve). In life position, with the ventral interarea and delthyrium resting against the substrate (Mancenido and Gourvennec, 2008), the sulci of both taxa would be located closer to the substrate than the anterior-most portions of the lateral gapes, thereby facilitating medially inhalant and laterally exhalant passive flow. Based on observations of flow patterns in living brachiopods, Rudwick (1970) suggested a

laterally-inhalant and medially-exhalant feeding current pattern for spiriferide brachiopods. Using gaping hollow models, Alexander (1999) demonstrated that both laterally-inhalant/medially-exhalant and medially-inhalant/laterally-exhalant passive flow are possible in *Paraspirifer bownockeri*, depending on the orientation of the shell with respect to incoming current. These observations indicate that both morphology and life orientation are important factors in determining if a particular shell form is an effective passive suspension feeding body plan.

Specimen Selection and Morphometric Methods:

Specimens

Samples of *Composita* from across the American Mid-Continent were obtained from the collections of the Yale Peabody Museum of Natural History. This material included specimens collected from Late Mississippian through Late Pennsylvanian strata from localities in Texas, Kentucky, and Iowa. Specimens with completely preserved shells and clearly visible growth lines ($n = 136$) were selected for morphometric analysis.

Morphometric methods

Three-dimensional Bookstein shape coordinates (after Bookstein 1986, 1991) were used to examine shape differences among the selected specimens. In both two and three dimensions, Bookstein shape

coordinates depict the relative positions of various anatomical landmarks within a shape coordinate space that is defined by aligning and scaling different specimens according to a shared set of measurements demarcated by the landmarks. Tyler and Leighton (2011) were the first workers to apply Bookstein shape coordinates to three-dimensional landmark data, and demonstrated the applicability of the technique for identifying shape changes in brachiopods. In three dimensions, Bookstein shape coordinates are calculated based on interlandmark measurements for tetrahedral configurations of landmarks. Three of the landmarks comprising the overall tetrahedral configuration define a triangular base plane, which allows all of the specimens being examined to be rotated to a common orientation (usually the x-y plane) in Euclidean space. Two of the base plane landmarks are further used to define a baseline dimension, which translates every specimen to a shared position when assigned to an axis in Euclidean space. Using interlandmark measurements, the Cartesian coordinates of each landmark are determined by solving for the vertices of an irregular tetrahedron. By dividing the Cartesian coordinates of each landmark by the baseline dimension of the corresponding specimen, and thereby scaling the baseline of every specimen to unity, size variation among all of the specimens is removed. The resulting Bookstein shape coordinates depict shape differences among the entire set of specimens.

A single tetrahedral configuration of landmarks (Figure 2.2) was defined in order to test for differences in the shape of the commissure among the chosen specimens of *Composita*. Landmarks A (posterior-most point of the pedicle foramen), B (lower-most point of the medial sulcus along the commissure), and C (anterior-most point along the flat lateral portion of the commissure) were chosen to define the base plane. Landmark D (ventral-most point of the parasulcus along the commissure) was chosen due to the fact that it is the point along the commissure that would be furthest from the substrate in life position. In three-dimensional shape coordinate space, landmark A occurs at the origin, landmark B occurs at (1, 0, 0), and landmark C lies at some point in the x-y plane. As a result, the position of landmark D in shape coordinate space depicts the displacement of the parasulcus (irrespective of size) from the pedicle foramen, medial sulcus, and lateral portion of the commissure. These data relate to different aspects of the shell morphology and function of *Composita* as follows: (1) The distribution of landmark D in shape coordinate space determines whether or not significant variation in shell morphology exists in *Composita*; (2) The relative stratigraphic position and size of each specimen comprising the shape coordinate distribution determine whether or not differences in shape are more strongly associated with (*i.e.*, indicative of) evolutionary or ontogenetic change, and; (3) The trend in the vertical displacement of landmark D (whether

evolutionary or ontogenetic) serves to help predict the potential functional significance of the observed shape variation. Although these landmarks are not homologous in the strict sense (as would be required in order to use morphometric characters for phylogenetic analysis), they are directly related to suspension feeding function, and therefore valuable for testing the hypothesis of this study.

Because of the bilateral symmetry of brachiopods, measurements for landmarks not lying on the anterior-posterior axis were typically taken from the right side of each specimen, unless the left side of the shell was significantly less worn. On the few occasions when measurements were collected from the left-side of the specimen, the shape coordinate data were reflected around the x-axis for appropriate comparison with right-side data.

Results (Morphometric Analysis):

As the methods discussed in the latter part of this paper were based on the outcome of the morphometric analysis described in the previous section, morphometric results are given herein, prior to description of model construction methods and flume testing protocols.

Size and shape changes

Shape coordinate data from the morphometric analysis of *Composita* show a single distribution characterized by displacement of

landmark D in the z-dimension (Figures 2.3 and 2.4). Given the presumed life position of *Composita*, the z-dimension of the shape coordinate space resulting from the morphometric analysis is approximately perpendicular to the substrate. Therefore, displacement of landmark D in the z-dimension corresponds to vertical displacement (relative to the substrate) of the parasulcus from the medial sulcus, pedicle foramen, and lateral commissure. Comparing the relative size and stratigraphic position of the corresponding specimens, a clear association between increasing shell size and increasing vertical displacement of the parasulcus is apparent; indeed, vertical displacement of the parasulcus scales roughly linearly with shell size during the early ontogeny of the genus (Figures 2.5 and 2.6). No distinct association between the displacement of the parasulcus and the relative stratigraphic position of corresponding specimens is apparent, with specimens from various time intervals intergrading with one another throughout the shape coordinate distribution. Shell growth is allometric (Figure 2.6).

Model Construction and Flume Testing Protocols:

Model construction

The morphometric analysis of *Composita* revealed a single shape distribution characterized by increasing vertical displacement of the parasulcus from the pedicle foramen, medial sulcus, and lateral portion of

the commissure (Figures 2.3 and 2.4). Strong association between shape and relative size indicates that the shell morphology of *Composita* changed throughout its ontogenetic history, with the parasulcus becoming increasingly more displaced from the rest of the commissure. To test the functional significance of this trend, three specimens (one from each shape-size subgroup) were chosen for comparative testing in the flume tank (Figure 2.7). 1:1 scale plastic models of each specimen were constructed using silicone molds and a transparent urethane casting resin (Figure 2.8). For each specimen, two-piece molds were constructed for both valves. The exterior surface of each valve was replicated by covering the opposing valve in plasticine, and pouring a silicone rubber (Smooth-On OOMOO 25) over the remaining exposed surface of the shell. Plasticine was then used to coat the first half of each mold to an approximately uniform thickness (representing the thickness of the original valve), after which a second volume of silicone rubber was poured to complete the second half of the mold. A transparent urethane resin (Smooth-On Crystal Clear 200) was used to cast each model valve. Following mixing and vacuum degassing, the liquid resin was slowly poured into each mold and allowed to cure at room temperature for 16 hours, then subsequently heat cured for one hour at 100 degrees Celsius. After curing, excess material was trimmed from the cast valves using a scalpel and rotary tool until matched pairs of dorsal and ventral valves fit

roughly together. 400 grit sandpaper was used to further smooth and finish the commissure of each valve until a close fit was achieved.

Rudimentary wire springs were used to hinge matched pairs of valves together (Figure 2.8A). Springs for each articulated model were constructed from single strands of 20 gauge copper wire, repeatedly bent and trimmed until an appropriate fit with the interior surface of both valves was achieved. A rotary tool was used to cut a small groove in the interior surface of each valve, thereby allowing the wire hinge spring to be securely glued to both valves. The spring loaded hinge structure was not intended to simulate the articulation of the organism, but rather allowed the gape of the articulated models to be easily adjusted for testing in the flume.

A simulated lophophore was constructed for the largest of the three model brachiopods (Figure 2.8B). This design was used to approximate the resistance to ambient water flow that would naturally be brought about by the soft tissues present within the mantle cavity of a living brachiopod. In brachiopods, the lateral and frontal cilia of the lophophore tentacles function to capture and reject suspended food particles, with the lateral cilia representing the smallest spaces through which water and suspended food particles are strained (Rudwick, 1970; Strathmann, 1973). Although different brachiopods show substantial variation in overall lophophore structure, the arrangement of tentacles along the brachial axis of the

lophophore is similar among most adult forms (Kuzmina and Malakhov, 2007). In general, two closely spaced offset rows of tentacles span the entire length of the brachial axis of the lophophore, with the tentacles and the particular morphology of the lophophore effectively segmenting the mantle cavity of the animal into discrete inhalant and exhalant chambers (Rudwick, 1970). Although no direct measurements for the typical spacing of lateral cilia in brachiopods are given in the published literature, estimates based on transmission electron microscopy images of the linguliform *Glottidia pyramidata* (Gilmour, 1981) indicate a value of 3-4 µm (Kuzmina and Malakhov, 2007). Similarly, Dhar *et al.* (1997) successfully used the 5-6 µm diatom *Chaetoceros muelleri* for their endoscopic study of feeding in the terebratulide brachiopods *Terebratulina septentrionalis* and *Terebratalia transversa*, indicating that the maximum spacing of the lateral cilia in these species is less than 5 µm. To approximate similar values for the spacing of lateral cilia as closely as possible, material from a 5 µm domestic water filter (typically available in 1 and 5 µm sizes) was used to construct the simulated lophophore.

Athyrididine brachiopods such as *Composita* possessed calcareous lophophore supports (spiralia) developed as a pair of conical spirals with laterally oriented apices (Alvarez and Rong, 2002). Two equally-sized cones of filter material were shaped to fit inside of the largest model, and affixed to a simple wire frame in a laterally-opposed orientation similar to

the arrangement of spiralia in *Composita* (Figure 2.9). As the space within the coils of the spiralia of a living brachiopod would have been an open conduit, ringed on the outside by the ciliated tentacles of the lophophore, a 7/32 " hole was drilled through the axis of each filter cone in order to permit passage of fluid.

Flume schematics and testing protocols

A one-way recirculating flume tank was used to examine flow patterns within and around the model brachiopods (Figure 2.10). Smooth plexiglass was used for the walls and floor of the flume in order to avoid localized variation in flow velocity due to differences in the shape and character (sorting, grain-size, etc.) of the channel. The channel of the flume measured 3.5 m long by 0.27 m wide, and was filled to a maintained depth of 0.23 m. A turbulence-reducing flow-straightener was placed immediately in front of the channel inlet during all experiments.

During all of the flow experiments, a single model brachiopod was placed in the middle of the flume channel, 1.25 m downstream of the channel inlet. For each experiment, the model brachiopod was secured in place with plasticine, and positioned such that its pedicle foramen and part of its dorsal valve were in contact with the substrate, simulating life position. All of the models were adjusted to have a gape of approximately 3-4 degrees, a value consistent with that of a silicified specimen of *Composita* preserved with its shell gaping (Figure 2.2). As athyridide

brachiopods had interlocking cyrtomatodont dentition (Alvarez and Rong, 2002), it would have been impossible for living *Composita* to gape more than 10-15 degrees without prior breakage of the hinge teeth (Carlson, 1989). Therefore, the gape of the experimental models agrees with physical constraints on living *Composita*. Recent terebratulide brachiopods, which also possess cyrtomatodont hinge teeth, similarly show gapes of less than 15 degrees (Carlson, 1989).

Each of the model brachiopods was tested using three different shell orientations: (1) Anterior-posterior axis parallel to direction of flow, anterior end of shell facing upstream, (2) Anterior-posterior axis parallel to direction of flow, anterior end of shell facing downstream, and (3) Anterior-posterior axis perpendicular to direction of flow. During each experimental trial, India ink was used to trace flow patterns around and through the model brachiopod at free-stream current velocities of 0.02, 0.04, and 0.06 m/s. These ambient current velocities were chosen to facilitate visualization of dye flow patterns, but are also velocities at which living brachiopods are known to feed (LaBarbera, 1977).

Three protocols were used to inject ink into the model brachiopods during the flow experiments. First, with no applied ambient current, a pipette was used to inject a small volume of ink into the "mantle cavity" of each model. After removing the pipette from the flume channel, patterns of ink flow out of the models were observed for all three shell orientations.

Second, under applied ambient currents of 0.02, 0.04, and 0.06 m/s, small volumes of dye were released from a pipette held approximately 6-8 cm upstream of the model brachiopods. The pipette used for these tests was long enough that its bulb remained above water level at all times, thereby minimizing upstream disruption of flow. This protocol was mainly used to observe how easily current entered the models under each of the three shell orientations. Third, using a submerged length of aquarium airline tubing, ink was injected 2-3 cm upstream of the model brachiopods at ambient flow velocities of 0.02, 0.04, and 0.06 m/s. The airline tubing was attached to the substrate of the flume channel, parallel to the direction of flow, for a length of 20-25 cm upstream of the model, and run up along the wall of the flume channel to where it was attached to an ink-filled pipette held above water level. This arrangement of the pipette and tubing was designed to further minimize upstream flow disruption. The open end of the tubing was held in place with plasticine, and positioned at the same height above the substrate as the sulcus of the model brachiopod being examined. This protocol allowed more detailed observation of flow patterns than was possible using the other techniques.

Data from these experiments relate to the hypothesis as follows: (1) Observations for each model serve as a comparative functional test of how morphological differences among the model brachiopods affect passive circulation performance and patterns of flow, (2) Changes in the

orientation of the models with respect to ambient flow serve to demonstrate how the passive circulation performance of each morphology is affected by differences in life position, and (3) Differences in passive flow performance among the model brachiopods indicate how the observed trends are related to ontogenetic change.

Results (Flume Tank Analysis):

Hollow model flow patterns

All three models were observed to show a medially-inhalant and laterally-exhalant pattern of passive flow circulation (Figure 2.11), however, the strength of the inhalant and exhalant currents was observed to change according to the orientation of the models with respect to the direction of ambient current flow. The following flow behaviours were observed when dye was injected into the hollow models prior to application of current in the flume channel (consistent in all three models for flow velocities of 0.02, 0.04, and 0.06 m/s):

(1) Anterior-posterior axis parallel to direction of ambient flow, anterior end facing upstream:

Gyrating flow within the shell, exiting from both lateral gapes. Fluid also exits from both parasulci in the case of the largest model. Laminar flow around the sides and over the top of the shell, with a zone of vortex shedding downstream of the shell (observed in all orientations).

(2) Anterior-posterior axis parallel to direction of ambient flow, anterior end facing downstream:

The same pattern as observed in (1), although somewhat diminished.

(3) Anterior-posterior axis perpendicular to direction of ambient flow:

Fluid exits from the downstream lateral gape and parasulcus, with no outflow from the medial sulcus.

More thorough observation of relative passive circulation performance was possible using the upstream pipette and submerged tubing injection protocols. The following flow behaviours were observed using these techniques (consistent for flow velocities of 0.02, 0.04, and 0.06 m/s):

(1) Anterior-posterior axis parallel to direction of ambient flow, anterior end facing upstream:

Flow enters through the medial sulcus and gyrates within the shell, exiting from both lateral gapes. No exhalant flow through the parasulci of the smallest model (Figure 2.11A). Intermittent exhalant flow through the parasulci of the medium-sized model (Figure 2.11B and 2.11C).

Continuous exhalant flow through the parasulci of the largest model (Figure 2.11D). Laminar flow around the sides and over the top of the shell, with a zone of vortex shedding downstream of the shell (observed in all orientations).

(2) Anterior-posterior axis parallel to direction of ambient flow, anterior end

facing downstream:

No passive flow circulation was induced.

(3) Anterior-posterior axis perpendicular to direction of ambient flow

(Figure 2.11E):

Flow enters through the upstream lateral gape, exiting from the downstream lateral gape and parasulcus.

Lophophore model flow patterns

The simulated lophophore caused changes in the behaviour of passive flow through the large model. In particular, due to the size and resistance of the two filter cones, no gyrating flow was observed within the shell. The following flow behaviours were observed with the simulated lophophore installed in the largest model (consistent for flow velocities of 0.02, 0.04, and 0.06 m/s):

(1) Anterior-posterior axis parallel to direction of ambient flow, anterior end facing upstream (Figure 12.11F):

Flow enters through the medial sulcus, passing through axial canal of each cone, and exiting through both lateral gapes. A small amount of flow that does not reach the middle of the shell (adjacent to the axial canal of either cone) passes above the anterior end of either filter cone, exiting through the parasulci. Laminar flow around the sides and over the top of the shell, with a zone of vortex shedding downstream of the shell (observed in all orientations).

(2) Anterior-posterior axis parallel to direction of ambient flow, anterior end facing downstream:

Flow enters through the upstream lateral gape, passing through the axial canal of each cone, and exiting through the downstream lateral gape and parasulcus. Flow that does not enter the axial canal of the upstream filter cone moves across the anterior end of the downstream filter cone, exiting through the downstream parasulcus and lateral gape.

(2) Anterior-posterior axis parallel to direction of ambient flow, anterior end facing downstream:

No passive flow circulation was induced.

Discussion:

The shell morphology of *Composita* appears to have functioned as an effective passive suspension feeding body plan. In North America, *Composita* probably existed as a single species with a high degree of intraspecific morphological variation throughout its entire evolutionary history. The specimens of *Composita* used in the morphometric analysis were labeled as three different species, namely: *C. subtilita*, *C. trinuclea*, and *C. subquadrata*. The fact that these putative species (inclusive of a range of shell sizes, stratigraphic intervals, and geographic provenances) form a single intergrading shape and size distribution would support the contention that North American *Composita* should be considered a

monospecific genus.

The ontogenetic history of the taxon reflects development of a complex commissure in association with increasing shell size. Specifically, as shells of *Composita* grow larger, the parasulci become more vertically displaced from the medial sulcus and the lateral gapes. This growth is allometric, thereby changing the shape of the shell over time (Figures 2.6 and 2.7).

Ontogenetic changes in the morphology of *Composita* have observable effects on both the streamlining of the shell, and its ability to passively circulate flow. When oriented with the anterior medial sulcus facing upstream, all three models of *Composita* demonstrated a medially-inhalant and laterally-exhalant pattern of passive flow circulation; however, exhalant flow from the parasulci was regularly observed only in the largest model, with intermittent occurrences in the medium-sized model. Development of the parasulci is associated with increasing shell size. As *Composita* grew, successively larger whorls would have been added to the lophophore and supporting spiralia cones within the medial region of the mantle cavity (Williams and Wright, 1961). In order to accommodate larger spiralia, the animal would have had to enlarge its mantle cavity. In *Composita*, this apparently was accomplished by increasing the vertical displacement of the parasulci from the other segments (medial sulcus and lateral gapes) of the commissure. By

increasing the size of the lophophore the animal would be able to passively circulate greater volumes of water, and therefore capture more food particles per given time interval, hence increasing its feeding efficiency.

Spiriferide brachiopods have laterally oriented spiralia similar to those seen in *Composita*, but generally lack parasulci. Spiriferides have strophic hinge lines, and well-developed dorsal and ventral interareas (Carter *et al.*, 2006), which likely rested against the substrate in life position (Mancenido and Gourvennec, 2008). Furthermore, taxa such as *Paraspirifer* and *Cyrtospirifer* have much flatter lateral commissures than *Composita*, and deeper sulci that cause pronounced curvature along the midline of dorsal valves. Growth of deep medial sulci in forms similar to these genera would not only accommodate additional spiralia whorls and larger lophophores, but also tend to recline the shell, such that in life position the flat, anterior-most sections of the lateral commissure would be set back above the medial sulcus, eliminating the need for parasulci or parasulcus-like features.

Based on the patterns observed in the lophophore model, the spirolophous lophophore geometry and parasulci of *Composita* appear to have had a streamlining effect on inhalant flow. In all brachiopods, the geometry of the lophophore separates the mantle cavity into distinct inhalant and exhalant chambers (Rudwick, 1970). In the hollow models,

incoming flow entered through the medial sulcus and gyrated within the interior of the shell until finally exiting through the lateral gapes, and additionally through the parasulci in the case of the larger models. In the lophophore model, however, only a small amount of incoming flow that was not diverted into the medial region of the shell and subsequently channeled through either lophophore cone into the lateral exhalant streams was diverted out of the shell through the parasulci (see arrow in Figure 2.11F, and "parasulcus outflow" in Figure 2.12). In terms of maintaining effective separation of the mantle cavity, the resistant filter material of the model lophophore forced much of the inhalant flow stream to move through the path of least resistance (the axial canal of each lophophore cone), focusing the lateral exhalant flow streams, and clearly dividing the mantle cavity into distinct inhalant and exhalant chambers. The nozzle-like effect that the model lophophore had on incoming flow contrasts with the freely gyrating flow observed in the mantle cavities of the hollow models, suggesting that the lophophore of *Composita* likely had similar resistant and streamlining effects on inhalant flow. Such a pattern, focusing inhalant flow and entrained food particles over the lophophore tentacles and their cilia, would be obviously beneficial in terms of passive suspension feeding.

The function of the streamlined parasulcate outflow observed in the lophophore model is not particularly clear. It is possible that the

parasulcate outflow streams helped to stabilize the lophophore tentacles, thereby maintaining constant resistance against the incoming inhalant flow stream. The lophophore of *Composita* was probably ringed by two rows of tentacles following the outline of the calcareous spiralia, as is the case with all modern spirolophous taxa. The lophophore tentacles would have maintained inhalant-exhalant division of the mantle cavity by extending themselves outward from the brachial axis of the lophophore, forming a permeable barrier against incoming flow. With the lophophore tentacles outstretched, the parasulcate outflow streams (exiting the mantle cavity from the gaps in between successive whorls of the lophophore) would tend to stabilize both rows of tentacles against the incoming inhalant flow stream, preventing tentacles from different whorls of the lophophore from overlapping one another.

Based on the flow patterns observed in the case of the lophophore model, it is also possible that the parasulci of *Composita* functioned as conduits for particle rejection. Although this interpretation is purely speculative, and not conclusive based on the data presented here, it is consistent with observations of feeding and particle rejection in living terebratulide brachiopods. Living *Terebratulina septentrionalis* and *Terebratalia transversa* exhibit laterally-inhalant and medially-exhalant feeding currents and reject most inedible detritus from the lateral arms of their plectolophous lophophores, where suspended particles first come in

contact with the lophophore (Dhar *et al.*, 1997). Similar behaviour would be plausible in the case of *Composita* due to the fact that the inhalant flow stream would contact the lophophore tentacles very close to the highest (ventral-most) point of either parasulcus, thereby allowing rapid rejection and immediate outflow of inedible particles, which would otherwise potentially be caught within the lophophore.

Under constant unidirectional flow, shells of *Composita* only show fully developed passive circulation when oriented with the anterior-posterior axis of the shell aligned parallel to the direction of flow and the medial sulcus facing upstream. This alignment probably constitutes the preferred life orientation of *Composita* and other morphologically similar athyridide brachiopods. As observed in both the hollow models and the lophophore model, *Composita* could not exploit passive flow when oriented with the anterior sulcus facing downstream. In this orientation, the animal would have had to expend more energy actively generating feeding currents than if it was simply rotated 180 degrees, with the sulcus facing upstream. Similarly, none of the experimental models showed medially-exhalant passive flow when oriented with the anterior-posterior axis of the shell oriented perpendicular to the direction of ambient flow. As a consequence, in this orientation *Composita* would have had to either arrest particle collection on the upstream half of the lophophore, or pump against ambient current in order

to avoid disruption of the upstream lophophore tentacles by incoming passive flow. Again, both of these alternatives would be less efficient than simply orienting the shell with the anterior sulcus facing upstream.

LaBarbera (1977) observed active reorientation in response to changing ambient flow directions in living *Laqueus californianus*. Living *Laqueus* have adjustor muscles that function to reorient the shell about the fixed pedicle stalk. To date, no workers have described pedicle adjustor muscle scars in *Composita*; however, this could potentially be due to their small size, and the fact that brachiopod shells with strongly interlocking cyrtomatodont dentition are infrequently preserved as single valves (Leighton, 2001), rather than true absence of the feature.

Throughout its ontogeny *Composita* was able to resorb shell material around the pedicle, increasing the size of the pedicle foramen and allowing larger animals to accommodate more rotund pedicle stalks (Figure 2.7). As a result, if *Composita* possessed pedicle adjustor muscles, it would easily be able to preferentially adjust its orientation with respect to ambient flow, in a manner similar to *Laqueus*, and therefore be capable of pointing the medial sulcus upstream so as to exploit fully developed passive flow.

Fully developed medially-inhalant and laterally-exhalant passive flow similar to that observed in *Composita* has been experimentally demonstrated in the case of the spiriferide brachiopods *Cyrtospirifer* and

Paraspirifer bownockeri (Wallace and Ager, 1966; Alexander, 1999; Shiino et al., 2009; Shiino, 2010). Athyridide and spiriferide brachiopods are both generally biconvex, and share laterally dispersed spiralia; corresponding morphology, passive circulation function, and life orientations in athyridides and spiriferides points to the strong influence of passive suspension feeding on the evolution and development of brachiopods, and probably benthic invertebrates in general.

Conclusion:

The shell morphology of *Composita* functioned as an effective passive suspension feeding body plan. North American examples of *Composita* appear to constitute a single species with an ontogenetic history reflecting increasing vertical displacement of the parasulci from the anterior medial sulcus, pedicle foramen, and lateral sections of the commissure, with increasing shell size. This growth pattern causes the lateral and parasulcate gapes to rest higher above the substrate than the medial sulcus gape when shells are in life position.

Fully developed passive flow occurs in *Composita* when shells are oriented in a unidirectional current with the anterior-posterior axis parallel to the direction of flow, and the anterior medial sulcus facing upstream. When hollow models are placed in this orientation, flow enters the shell through the medial sulcus and gyrates within the mantle cavity, exiting

from both lateral gapes. Flow exited from the parasulcate gapes continuously in the largest model of *Composita* tested (27.45 mm anterior-posterior length), and sporadically in the case of an intermediately-sized model (21.56 mm anterior-posterior length).

Installation of a simulated lophophore in the largest model resulted in visible streamlining of flow inside the mantle cavity. Specifically, after entering the shell through the medial sulcus, most of the inhalant flow stream was immediately diverted through the lophophore cones, exiting through the lateral gapes. The small amount of inhalant flow that did not reach the middle of the shell (adjacent to the center of either lophophore cone) passed above the anterior end of either filter cone, exiting through the parasulci. No gyrating flow was observed within the mantle cavity of the lophophore model. Differences in passive fluid circulation observed using the lophophore model illustrate the importance of attempting to replicate some degree of the resistance to flow brought about by soft tissue structures when performing hydrodynamic experiments with model shells.

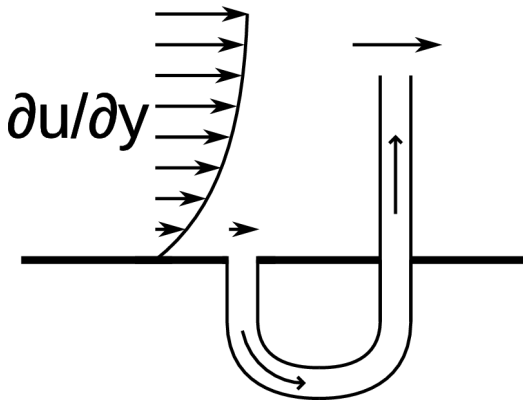


Figure 2.1 (modified after Vogel 1994):

The effect of viscous entrainment. Fluid viscosity and the no-slip condition create vertical velocity gradients ($\partial u / \partial y$) in flows where they encounter solid objects. Any organism with a body plan that approximates a vertically-oriented piping system will be able to passively circulate fluid through itself due to the higher flow velocity near the exhalant opening. Viscous entrainment will have the same effect on flow through the pipe irrespective of the ambient flow direction.

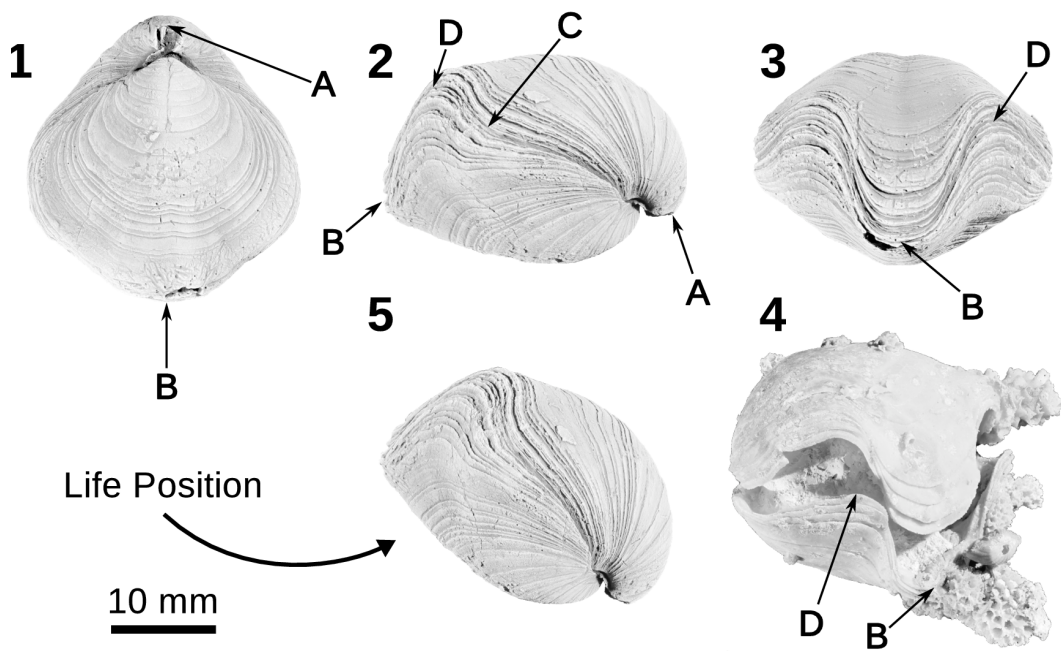


Figure 2.2:

Landmarks used for morphometric analysis of *Composita*. 1, 2, and 3: dorsal, lateral, and anterior aspects of shell (YPM 577746). 4: gaping articulated specimen (YPM 519279) (heavily encrusted). 5: specimen in inferred life position (YPM 577746). (A): posterior-most point of pedicle foramen. (B): lower-most point of the medial sulcus along commissure. (C): anterior-most point along flat lateral portion of commissure. (D): ventral-most point of parasulcus along commissure.

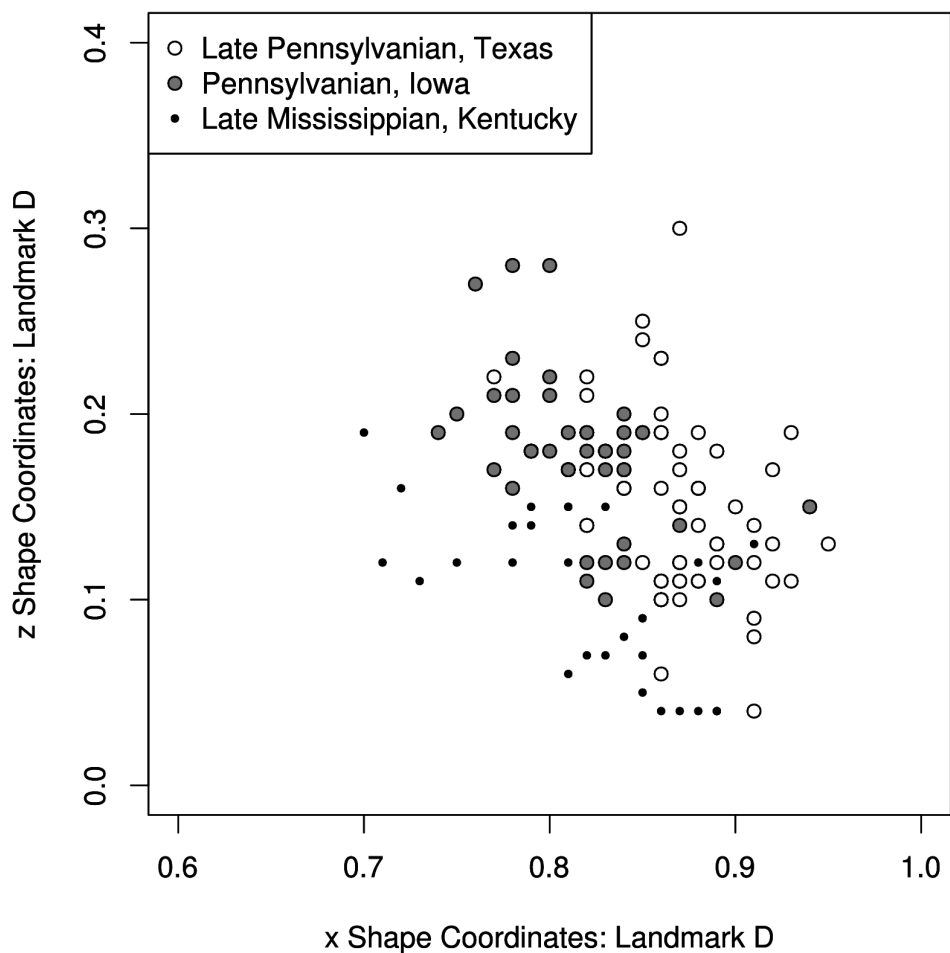


Figure 2.3:

Z and X shape coordinates of landmark D. On these axes the shape distribution shows vertical and forward displacement of the landmark. Note intergradational distribution of specimens from different localities and stratigraphic intervals.

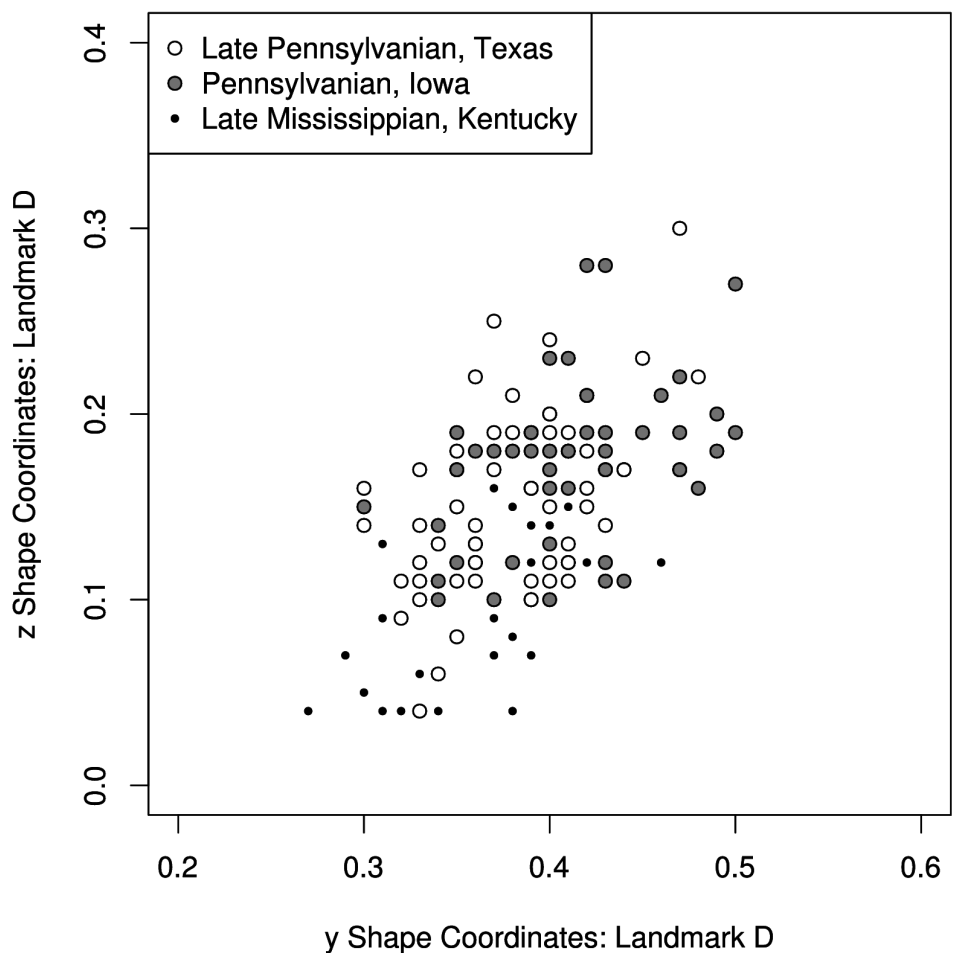
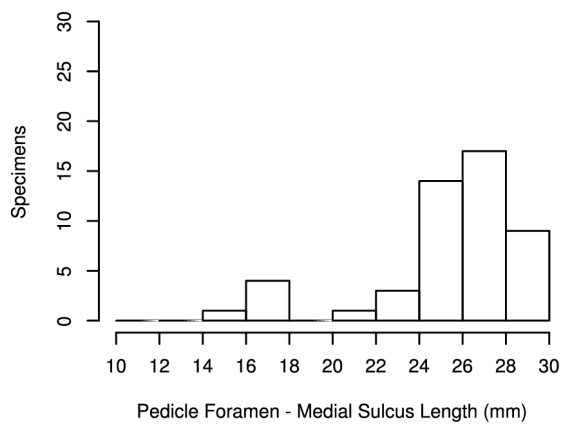


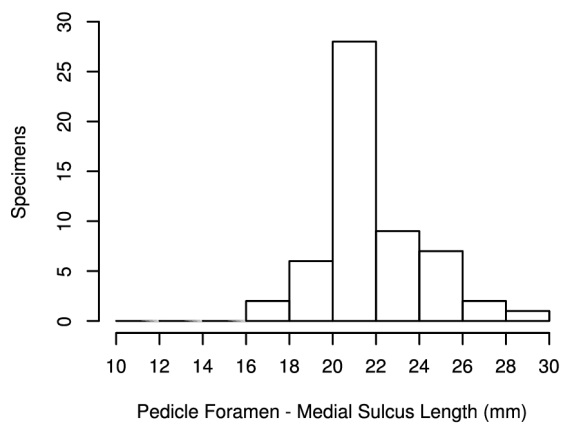
Figure 2.4:

Z and Y shape coordinates of landmark D. On these axes the shape distribution shows vertical and lateral displacement of the landmark. Note intergradational distribution of specimens from different localities and stratigraphic intervals.

Late Pennsylvanian, Texas



Pennsylvanian, Iowa



Late Mississippian, Kentucky

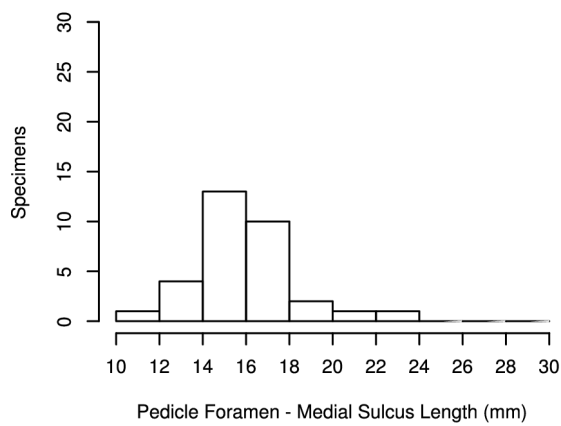


Figure 2.5:

Size and shape variation among samples of *Composita*. The three samples (Late Mississippian, Kentucky; Pennsylvanian, Iowa; Late Pennsylvanian, Texas) appear to indicate geographical variation in shape when plotted independently, however, sampling bias is apparent when size distributions for each sample are compared. Comparing the shape distributions for landmark D (Figures 2.3 and 2.4) to the size distributions of the corresponding samples, an association between increasing shell size and increasing vertical displacement of the landmark is apparent, indicating an ontogenetic shape-change trend.

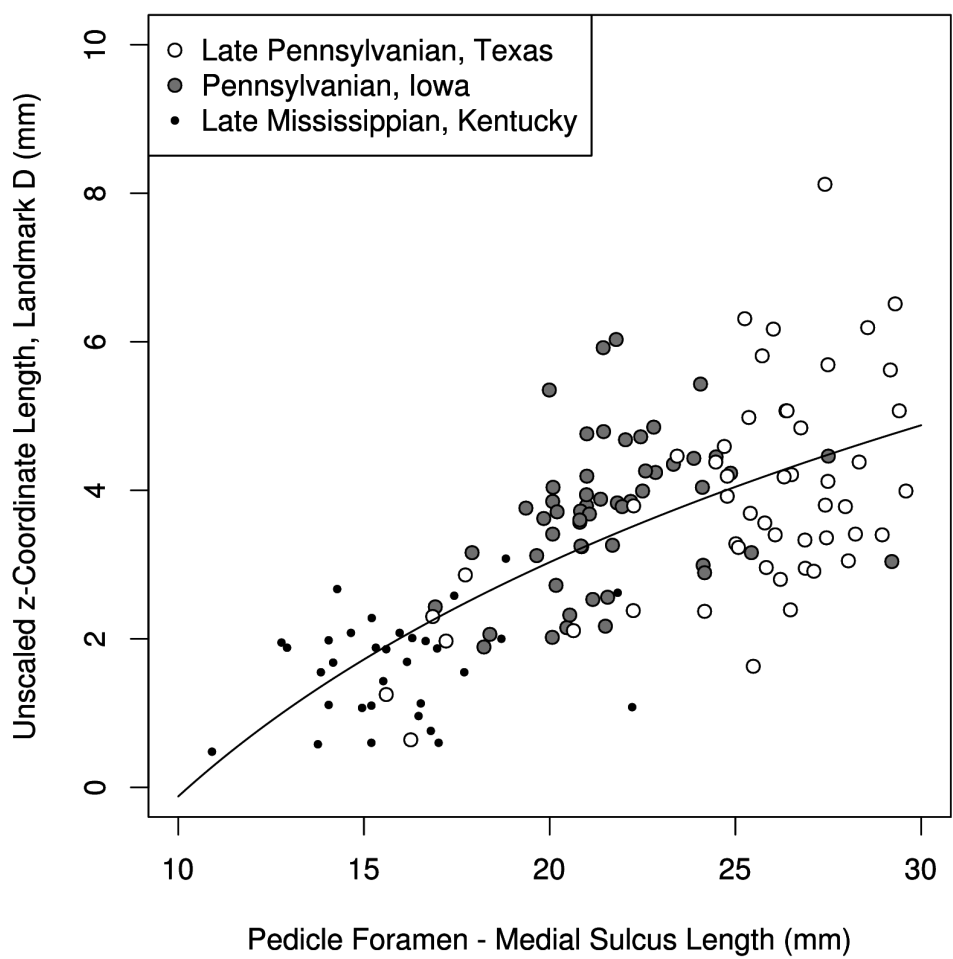


Figure 2.6:

Allometric growth in *Composita*. The displacement of landmark D in the z-dimension increases throughout ontogeny. Given the presumed life position of *Composita*, the z-dimension is approximately perpendicular to the substrate. Therefore, displacement of landmark D in the z-dimension corresponds to vertical displacement (relative to the substrate) of the parasulcus from the medial sulcus, pedicle foramen, and lateral commissure. Logarithmic curve fit (non-linear least squares regression): $y = -10.60 + 4.55\ln(x)$, Adjusted $R^2 = 0.48$, $p < 0.01$.

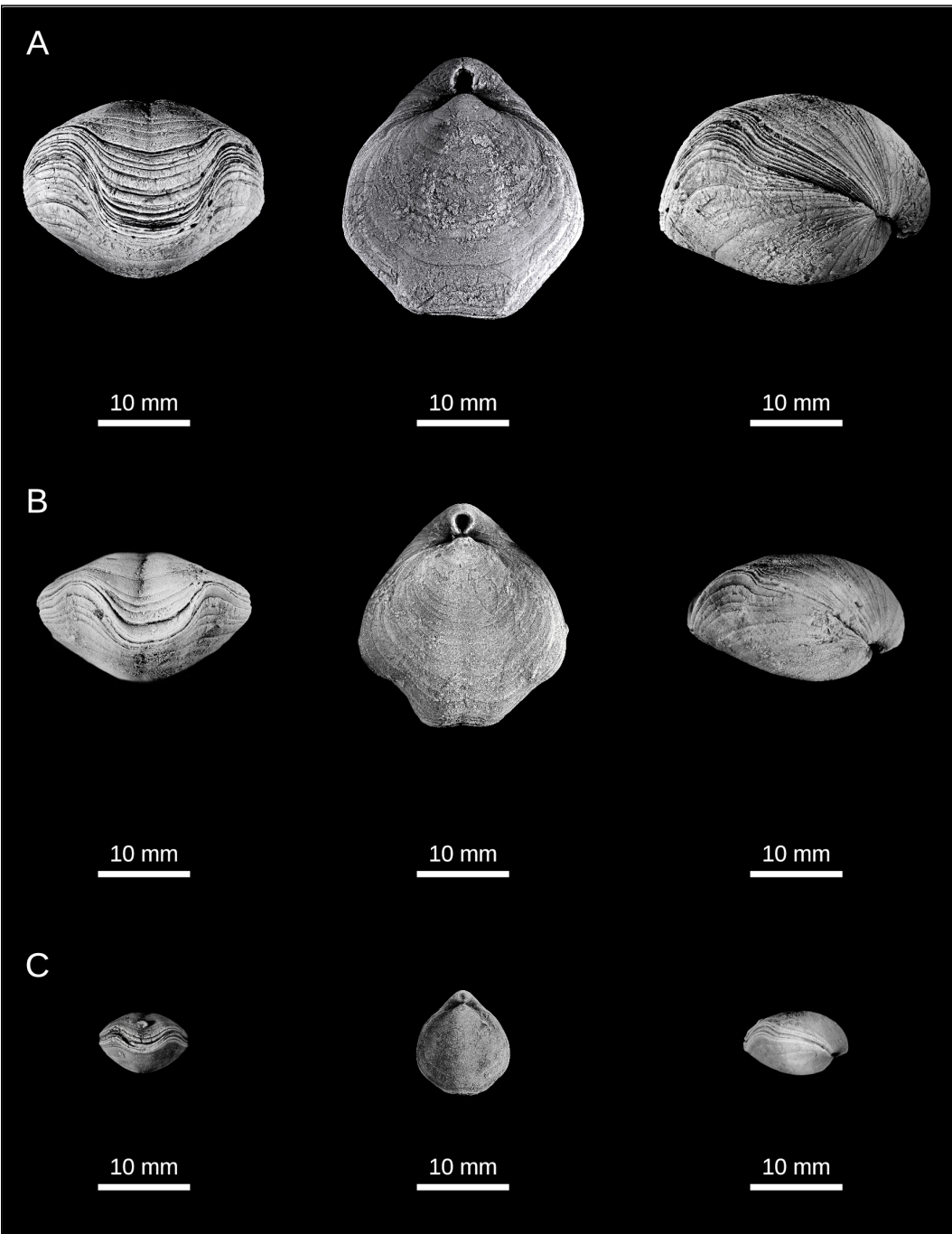


Figure 2.7:

Specimens of *Composita* used to construct models for use in flume tank experiments. (A): YPM 519088, Late Pennsylvanian, Texas; (B): YPM 147214, Pennsylvanian, Iowa; (C): YPM 403163, Late Mississippian, Kentucky.

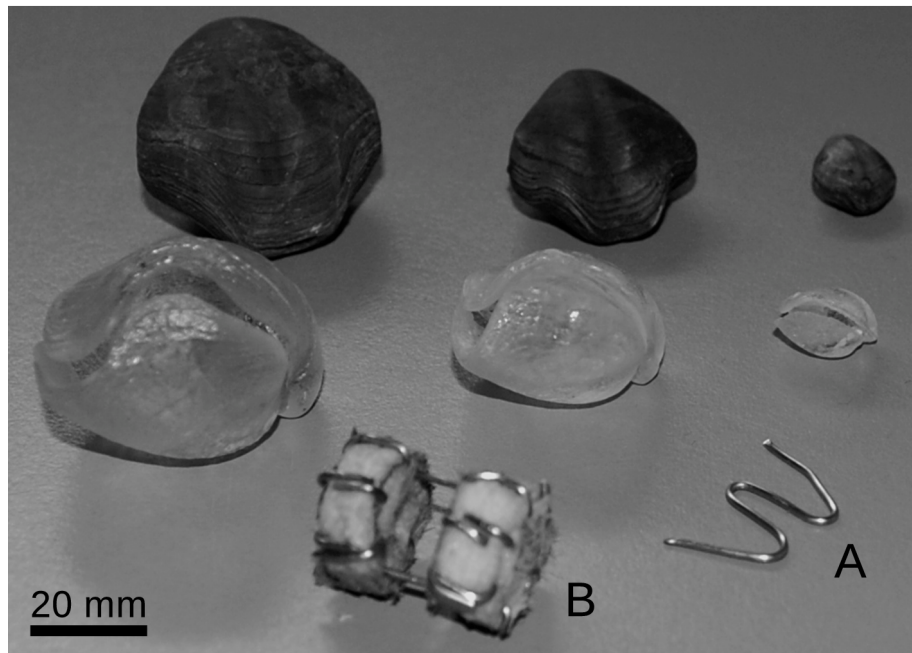


Figure 2.8:

Specimens, models, and model components used in flume experiments.

(A): example of rudimentary spring used to hinge valves together; (B):

simulated lophophore used in the largest model.

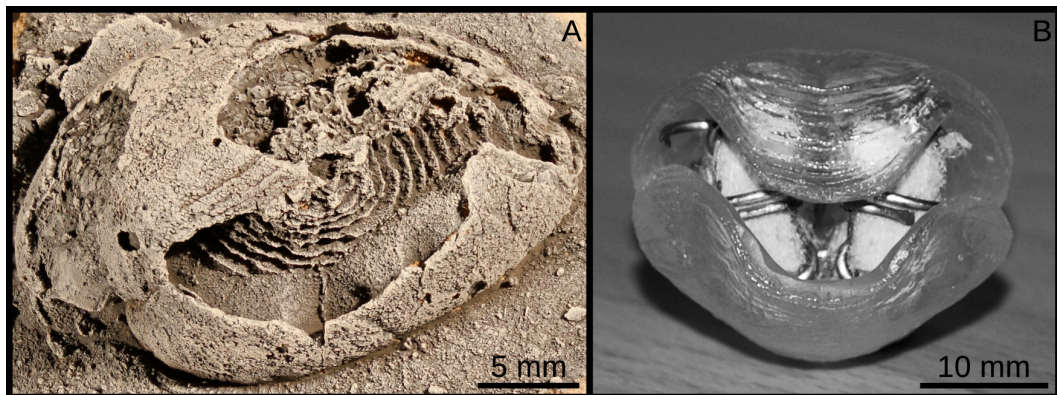


Figure 2.9:

(A): articulated specimen of *Composita* with external mold of spiralia preserved inside the shell. (YPM 236752, Late Pennsylvanian, Nevada). Anterior end of shell towards right side of figure. (B): large model of *Composita* with simulated lophophore installed.

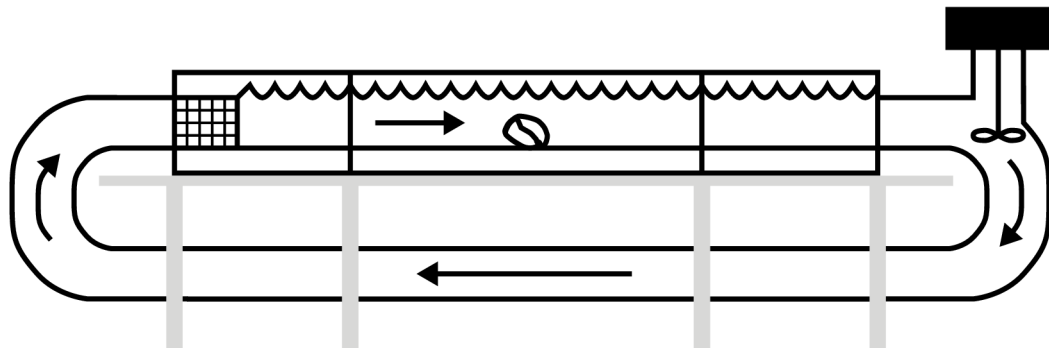
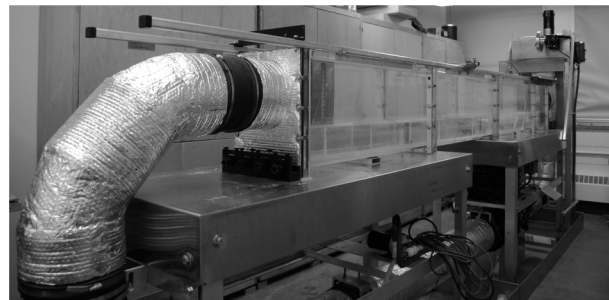
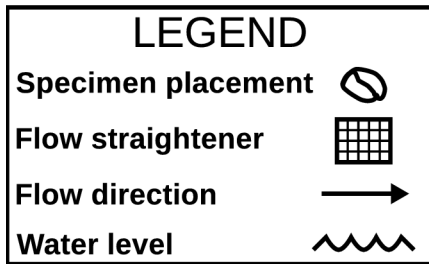


Figure 2.10:

Flume tank used for study of passive flow in *Composita*. During all experiments, models were placed in the middle of the flume channel, 1.25 m downstream of the channel inlet (demarcated by upstream end of flow straightener).

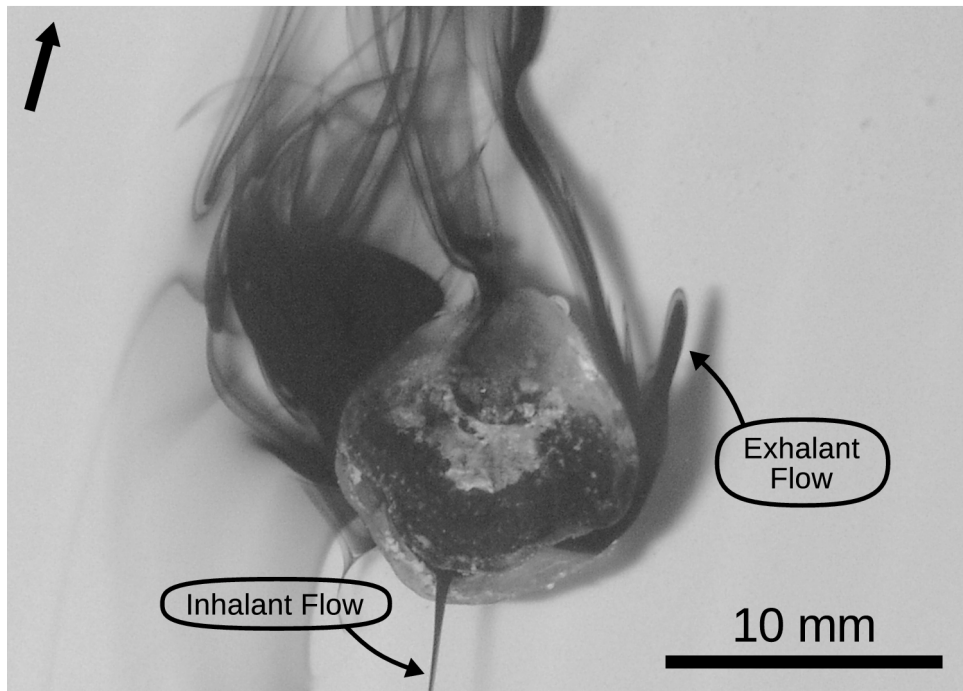


Figure 2.11:

Small hollow model of *Composita* showing medially-inhalant and laterally-exhalant passive flow (0.06 m/s unidirectional current). Note absence of parasulcate outflow streams. Anterior-posterior axis of shell parallel to direction of flow. Flow direction demarcated by thick black arrow.

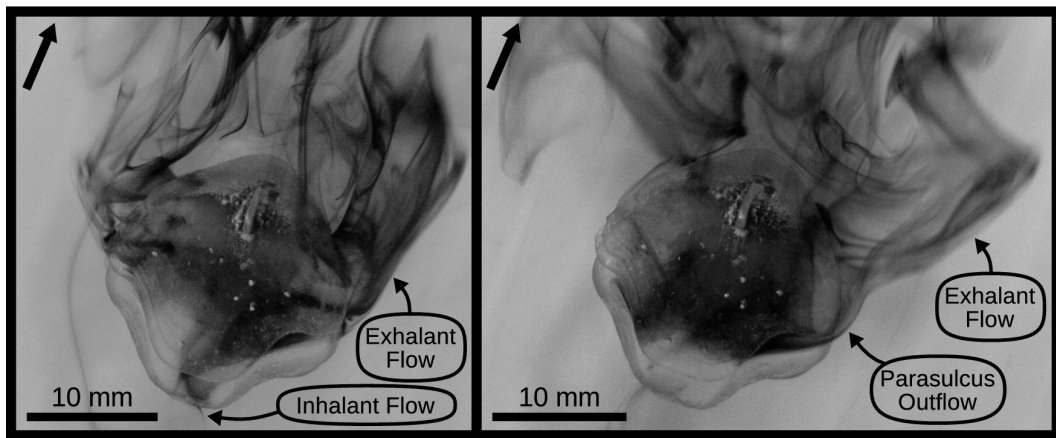


Figure 2.12:

Intermediately-sized hollow models showing medially-inhalant and laterally-exhalant passive flow (0.06 m/s unidirectional current). Note intermittent parasulcate outflow stream. Anterior-posterior axis of shell parallel to direction of flow. Flow direction demarcated by thick black arrows.

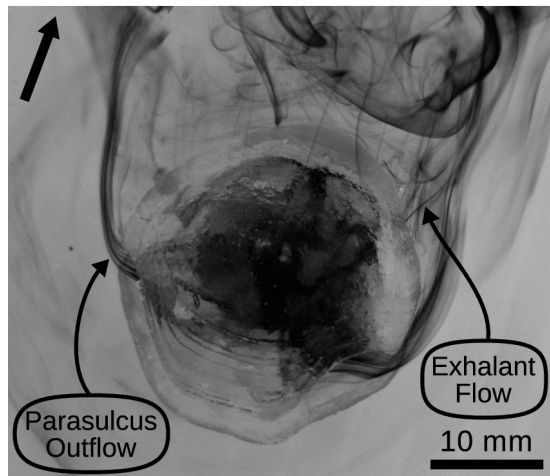


Figure 2.13:

Large hollow model showing medially-inhalant and laterally-exhalant passive flow, with vigorous outflow from both parasulci (0.06 m/s unidirectional current). Anterior-posterior axis of shell parallel to direction of flow. Flow direction demarcated by thick black arrow.

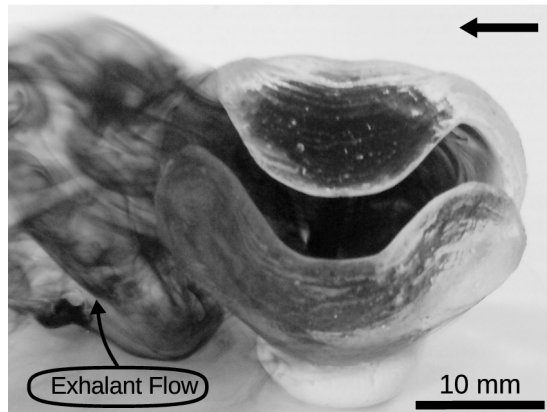


Figure 2.14:

Large hollow model showing laterally-inhalant (upstream) and laterally-exhalant (downstream) passive flow (0.06 m/s unidirectional current). Shell oriented with anterior-posterior axis perpendicular to direction of flow. Flow direction demarcated by thick black arrow. Note absence of exhalant flow from medial sulcus.

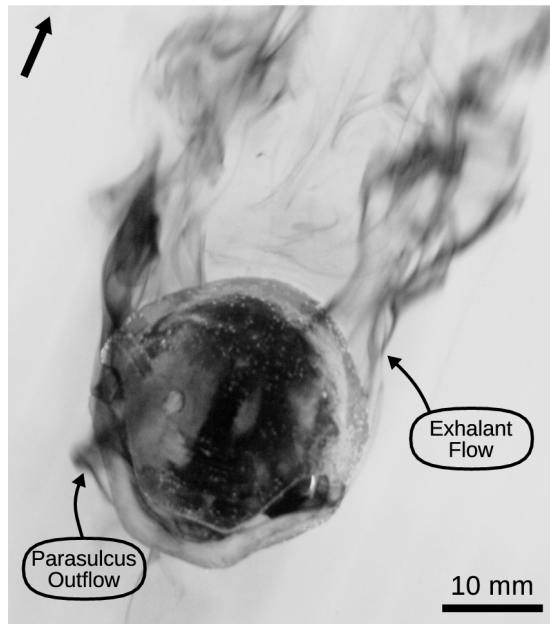


Figure 2.15:

Large model with simulated lophophore installed. Note streamlined medially-inhalant and laterally-exhalant passive flow (0.06 m/s unidirectional current). Note small, intermittent parasulcate outflow stream, shown exiting from left parasulcus. Anterior-posterior axis of shell parallel to direction of flow. Flow direction demarcated by thick black arrow.

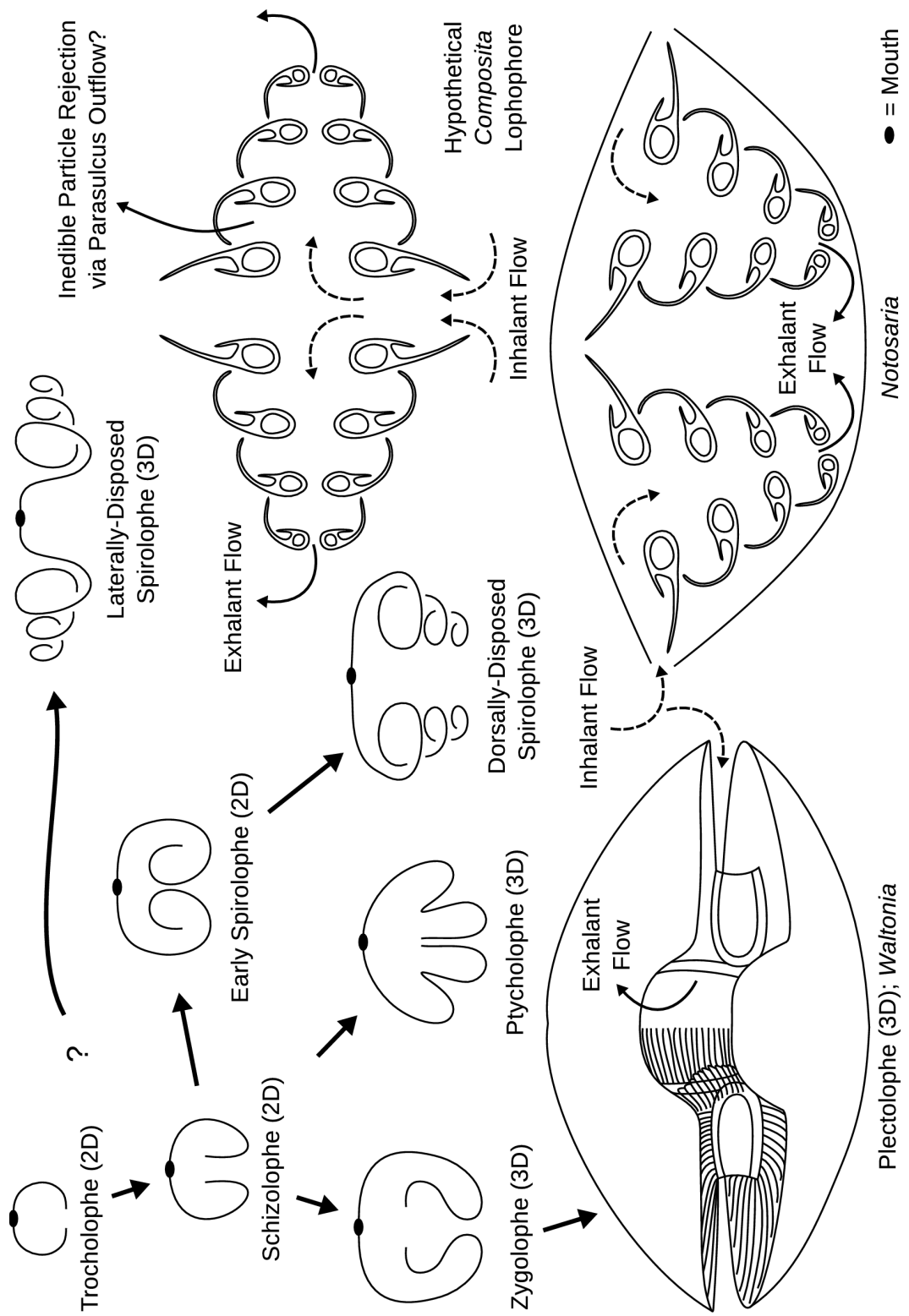


Figure 2.16 (modified after Rudwick 1970; Kuzmina and Malakhov 2007): Generalized ontogenetic pathways and brachial axis geometries of rhynchonelliform brachiopod lophophores (arrows do not indicate any phylogenetic relationship). Development of the lophophore entails an increase in geometric complexity as the organ grows from an essentially flat, two-dimensional structure into a more complex three-dimensional form. Tentacle arrangement and flow patterns for *Waltonia* and *Notosaria* based on observations by Rudwick (1970). Hypothetical tentacle arrangement shown for *Composita* is based on uniformitarian analogy with *Notosaria*. An alternative tentacle arrangement for laterally-disposed spirolophes is given by Williams and Wright (1961). Speculative particle rejection via parasulcus outflow proposed for *Composita* based on analogy with behaviour of living *Terebratulina* and *Terebratalia* observed by Dhar *et al.* (1997).

References:

- Alexander, R. R. 1999. Function of external skeletal characteristics of articulate brachiopods. Pp. 371-398 *in* E. Savazzi, ed. Functional morphology of the invertebrate skeleton. John Wiley & Sons, New York.
- Alexander, R. R. 2001. Functional morphology and biomechanics of articulate brachiopod shells. Pp. 145-170 *in* S.J. Carlson and M.R. Sandy, eds. Brachiopods ancient and modern, a tribute to G. Arthur Cooper. The paleontological society papers, volume 7.
- Alvarez, F., and J. Rong. 2002. Athyridida. Pp. H1475-H1604 *in* A. Williams et al. Brachiopoda 4, Rhynchonelliformea (part). Part H of R. L. Kaesler, ed. Treatise on invertebrate paleontology. Geological Society of America, Boulder, and University of Kansas, Lawrence.
- Alvarez, F., J. Rong, and A. J. Boucot. 1998. The classification of athyridid brachiopods. Journal of Paleontology 72:827-855.
- Bookstein, F. L. 1986. Size and shape spaces for landmark data in two

dimensions. Statistical Science 1:181-242.

Bookstein, F. L. 1991. Morphometric tools for landmark data: geometry and biology. Cambridge University Press, Cambridge.

Burk, C. A. 1954. Faunas and age of the Amsden Formation in Wyoming. Journal of Paleontology 28:1-16.

Carlson, S. J. 1989. The articulate brachiopod hinge mechanism: morphological and functional variation. Paleobiology 15:364-386.

Carlson, S. J., and L. R. Leighton (2004) Incorporating stratigraphic data in the phylogenetic analysis of the Rhynchonelliformea. Pp. 248-258 *in* Brunton, C. H. C., L. R. M. Cocks, and S. L. Long, eds. Brachiopods past and present. The systematics association special volume series 63.

Carter, J. L., J. G. Johnson, R. Gourvennec, and H. Hong-Fei. 2006. Spiriferida. Pp. H1689-H1876 *in* A. Williams et al. Brachiopoda 5, Rhynchonelliformea. Part H of R. L. Kaesler, ed. Treatise on invertebrate paleontology. Geological Society of America,

Boulder, and University of Kansas, Lawrence.

Dhar, S. R., A. Logan, B. A. MacDonald, and J. E. Ward. 1997.

Endoscopic investigations of feeding structures and mechanisms in two plectolophous brachiopods. Invertebrate Biology 116:142-150.

Gilmour, T. H. J. 1981. Food-collecting and waste-rejecting mechanisms in *Glottidia pyramidata* and the persistence of lingulacean inarticulate brachiopods in the fossil record. Canadian Journal of Zoology 59:1539-1547.

Grinnell, R. S., and G. W. Andrews. 1964. Morphologic studies of the brachiopod genus *Composita*. Journal of Paleontology 38:227-248.

Kuzmina, T. V., and V. V. Malakhov. 2007. Structure of the brachiopod lophophore. Paleontological Journal 41:520-536.

LaBarbera, M. 1977. Brachiopod orientation to water movement 1. Theory, laboratory behavior, and field orientations. Paleobiology 3:270-287.

LaBarbera, M. 1984. Feeding currents and particle capture mechanisms in suspension feeding animals. American Zoologist 24:71-84.

Leighton, L. R. 2001. New directions in the paleoecology of Paleozoic brachiopods. Pp. 185-205 in S. J. Carlson and M. R. Sandy, eds. Brachiopods ancient and modern, a tribute to G. Arthur Cooper. The paleontological society papers, volume 7.

Leighton, L. R., and C. L. Schneider. 2008. Taxon characteristics that promote survivorship through the Permian-Triassic interval: transition from the Paleozoic to the Mesozoic brachiopod fauna. Paleobiology 34:65-79.

Leys, S. P., G. Yahel, M. A. Reidenbach, V. Tunnicliffe, U. Shavit, and H. Reiswig. 2011. The sponge pump: the role of current induced flow in the design of the sponge body plan. PLoS ONE. e27787

Lutz-Garihan, A. B. 1976. *Composita subtilita* (Brachiopoda) in the Wreford megacyclothem (Lower Permian) in Nebraska, Kansas, and Oklahoma. The University of Kansas Paleontological Contributions 81:1-21.

Mancenido, M. O., and R. Gourvennec. 2008. A reappraisal of feeding current systems inferred for spire-bearing brachiopods. *Earth and Environmental Science Transactions of the Royal Society of Edinburgh* 98:345-356.

Prandtl, L., and O. G. Tietjens. 1934. Applied hydro- and aeromechanics. Dover, New York.

Rudwick, M. J. S. 1970. Living and fossil brachiopods. Hutchinson University Library, London.

Shiino, Y. 2010. Passive feeding in spiriferide brachiopods: an experimental approach using models of Devonian *Paraspirifer* and *Cyrtospirifer*. *Lethaia* 43:223-231.

Shiino, Y., O. Kuwazuru, and N. Yoshikawa. 2009. Computational fluid dynamics simulations on a Devonian spiriferid *Paraspirifer bownockeri* (Brachiopoda): generating mechanism of passive feeding flows. *Journal of Theoretical Biology* 259:132-141.

Strathmann, R. 1973. Function of lateral cilia in suspension feeding of

lophophorates (Brachiopoda, Phoronida, Ectoprocta). Marine Biology 23:129-136.

Sutherland, P. K., and F. H. Harlow. 1967. Late Pennsylvanian brachiopods from north-central New Mexico. Journal of Paleontology 41:1065-1089.

Tyler, C. L., and L. R. Leighton. 2011. Detecting competition in the fossil record: support for character displacement among Ordovician brachiopods. Palaeogeography, Palaeoclimatology, Palaeoecology 307:205-217.

Van Valen, L. 1976. Ecological species, multispecies, and oaks. Taxon 25:233-239.

Vogel, S. 1974. Current-induced flow through the sponge, *Halichondria*. The Biological Bulletin 147:443-456.

Vogel, S. 1994. Life in moving fluids: the physical biology of flow. Second edition. Princeton University Press, Princeton.

Vogel, S., and W. L. Bretz. 1972. Interfacial organisms: passive ventilation

in the velocity gradients near surfaces. *Science* 175:210-211.

Wallace, P., and D. V. Ager. 1966. Demonstration: flume experiments to test the hydrodynamic properties of certain spiriferid brachiopods with reference to their supposed life orientation and mode of feeding. *Proceedings of the Geological Society of London* 1635:160-163.

Williams, A., and A. D. Wright. 1961. The origin of the loop in articulate brachiopods. *Palaeontology* 4:149-176.

CONCLUSIONS

Geometric morphometrics and experimental fluid dynamics can be meaningfully and pragmatically applied to questions about the functional morphology of marine organisms. Morphometric analysis provides a framework for establishing patterns of morphological variation, while tests of function are the basis for identifying how the observed patterns of morphological variation relate to an organism's life mode.

When the relevant caveats (landmark selection, choice of baseline/baseplane, etc.) are taken into account, the method of Bookstein shape coordinates is an effective and logically convenient technique for three-dimensional analysis of morphological variation within and among samples. Size and shape data from a shape coordinate analysis can be used in association with statistical tests of difference and a variety of categorical data (taxon, stratigraphic position, geographical provenance, etc.) to make useful inferences about patterns of morphological variation.

The shell morphology of *Composita* functioned as an effective passive suspension feeding body plan. North American examples of *Composita* probably constitute a single species with a significant degree of intraspecific morphological variation representative of an allometric ontogenetic history. The ontogeny of *Composita* involves differentiation of the commissure into vertically displaced parasulcate, lateral, and sulcate gapes. In life position, the parasulcate gapes are displaced farthest from

the substrate, followed by the lateral gapes, and anterior medial sulcus, respectively. In a unidirectional current, *Composita* shows fully developed passive fluid circulation when oriented with the anterior-posterior axis of the shell parallel to the direction of flow, and the anterior medial sulcus facing upstream. In this orientation, hollow models of *Composita* show medially-inhalant and laterally-exhalant passive flow, with more vigorous fluid circulation occurring in larger shells. In hollow models, inhalant flow freely gyrates within the shell before being exhaled through the lateral gapes. Flow exited the mantle cavity via the parasulcate gapes continuously in the largest hollow model of *Composita* (27.45 mm anterior-posterior length), and periodically in the case of the intermediately-sized model (21.56 mm anterior-posterior length). Installation of a simulated lophophore in the largest model of *Composita* visibly streamlined flow within the shell, focusing the lateral exhalant flow streams and eliminating the gyrating flow observed in the hollow models. The lophophore geometry of living *Composita* likely streamlined the mantle cavity in the same manner, concentrating inhalant flow and food particles over the lophophore tentacles and cilia. These observations suggest that passive feeding had an important influence on the development and evolution of *Composita*, and probably brachiopods in general.